

This PDF file is subject to the following conditions and restrictions:

Copyright © 2009, The Geological Society of America, Inc. (GSA). All rights reserved.
Copyright not claimed on content prepared wholly by U.S. government employees within scope of their employment. Individual scientists are hereby granted permission, without fees or further requests to GSA, to use a single figure, a single table, and/or a brief paragraph of text in other subsequent works and to make unlimited copies for noncommercial use in classrooms to further education and science. For any other use, contact Copyright Permissions, GSA, P.O. Box 9140, Boulder, CO 80301-9140, USA, fax 303-357-1073, editing@geosociety.org. GSA provides this and other forums for the presentation of diverse opinions and positions by scientists worldwide, regardless of their race, citizenship, gender, religion, or political viewpoint. Opinions presented in this publication do not reflect official positions of the Society.

This file may not be posted on the Internet.

Integrated sequence stratigraphy of the postimpact sediments from the Eyreville core holes, Chesapeake Bay impact structure inner basin

**James V. Browning
Kenneth G. Miller**

Department of Earth and Planetary Sciences, Rutgers University, Piscataway, New Jersey 08854, USA

Peter P. McLaughlin Jr.

Delaware Geological Survey, University of Delaware, DGS Building, 257 Academy Street, Newark, Delaware 19716, USA

Lucy E. Edwards

U.S. Geological Survey, 926A National Center, Reston, Virginia 20192, USA

Andrew A. Kulpecz

Department of Earth and Planetary Sciences, Rutgers University, Piscataway, New Jersey 08854, USA

David S. Powars

U.S. Geological Survey, 926A National Center, Reston, Virginia 20192, USA

Bridget S. Wade

Department of Geology and Geophysics, Texas A&M University, College Station, Texas 77843, USA

Mark D. Feigenson

James D. Wright

Department of Earth and Planetary Sciences, Rutgers University, Piscataway, New Jersey 08854, USA

ABSTRACT

The Eyreville core holes provide the first continuously cored record of postimpact sequences from within the deepest part of the central Chesapeake Bay impact crater. We analyzed the upper Eocene to Pliocene postimpact sediments from the Eyreville A and C core holes for lithology (semiquantitative measurements of grain size and composition), sequence stratigraphy, and chronostratigraphy. Age is based primarily on Sr isotope stratigraphy supplemented by biostratigraphy (dinocysts, nannofossils, and planktonic foraminifers); age resolution is approximately ± 0.5 Ma for early Miocene sequences and approximately ± 1.0 Ma for younger and older sequences. Eocene–lower Miocene sequences are subtle, upper middle

to lower upper Miocene sequences are more clearly distinguished, and upper Miocene–Pliocene sequences display a distinct facies pattern within sequences. We recognize two upper Eocene, two Oligocene, nine Miocene, three Pliocene, and one Pleistocene sequence and correlate them with those in New Jersey and Delaware. The upper Eocene through Pleistocene strata at Eyreville record changes from: (1) rapidly deposited, extremely fine-grained Eocene strata that probably represent two sequences deposited in a deep (>200 m) basin; to (2) highly dissected Oligocene (two very thin sequences) to lower Miocene (three thin sequences) with a long hiatus; to (3) a thick, rapidly deposited (43–73 m/Ma), very fine-grained, biosiliceous middle Miocene (16.5–14 Ma) section divided into three sequences (V5–V3) deposited in middle neritic paleoenvironments; to (4) a 4.5-Ma-long hiatus (12.8–8.3 Ma); to (5) sandy, shelly upper Miocene to Pliocene strata (8.3–2.0 Ma) divided into six sequences deposited in shelf and shoreface environments; and, last, to (6) a sandy middle Pleistocene paralic sequence (~400 ka). The Eyreville cores thus record the filling of a deep impact-generated basin where the timing of sequence boundaries is heavily influenced by eustasy.

INTRODUCTION

Previous coring, logging, and geophysical studies of the U.S. Mid-Atlantic margin (Fig. 1) have resulted in several major accomplishments. One was to establish this region as a natural laboratory for extracting global sea-level change from the stratigraphic record and evaluating the role of eustasy, tectonic subsidence, and sediment input on passive continental sedimentation (Fig. 1A; e.g., Miller and Mountain, 1994; Miller *et al.*, 1996, 1997, 2004; Kominz *et al.*, 1998, 2008; Kominz and Pekar, 2001; Browning *et al.*, 2006, 2008). Another accomplishment was recognition that the Chesapeake Bay region was underlain by a major impact structure known as the Chesapeake Bay impact structure (e.g., Poag *et al.*, 1994, 2004; Koeberl *et al.*, 1996; Poag, 1997) and that this impact structure overprinted the stratigraphic evolution and hydrologic resources of this region (e.g., Powars and Bruce, 1999). The primary focus of this contribution is to identify and date postimpact sequences (genetically related units bounded by unconformities and their correlative conformities; modified from Mitchum *et al.*, 1977 by Miller *et al.*, 1997) in the International Continental Scientific Drilling Program (ICDP)–U.S. Geological Survey (USGS) Eyreville, Virginia, core holes and to evaluate the facies and attendant depositional environmental changes.

The late Eocene Chesapeake Bay impact structure is an 85–90-km-diameter crater located on the U.S. Mid-Atlantic margin (Fig. 1), and it is the seventh largest and one of the best preserved of the known impact craters on Earth (for overview, see Sanford *et al.*, 2004). It is the second largest of a group of well-preserved marine impact structures that includes the Mjølnir (Norway), Montagnais (Canada), Lockne (Sweden), Kamensk (Russia), and Chicxulub (Mexico) structures (Ormö and Lindström, 2000). The Chesapeake Bay impact structure is half the size of Chicxulub but twice the size of other recognized marine craters. The complex Chesapeake Bay impact structure formed

at 35.4 Ma when an impactor hit the U.S. Atlantic continental shelf in the area now occupied by parts of Chesapeake Bay and adjacent regions (Fig. 1B; Powars *et al.*, 1993; Poag *et al.*, 1994, 2004; Koeberl *et al.*, 1996; Poag, 1997; Powars and Bruce, 1999; age estimate is derived by correlation to Chron C16n.1n by Pusz *et al.*, 2009). The Chesapeake Bay impact structure consists of a 38-km-diameter central basin surrounded by a 24-km-wide annular trough (Fig. 1). The central basin has a central uplift surrounded by a moat. The entire structure is buried by ~500 m of postimpact upper Eocene–Recent coastal plain and continental shelf sediments that are thickest in the moat (Powars and Bruce, 1999; Poag *et al.*, 2004; Kulpecz *et al.*, this volume).

Recognizing the scientific importance of the Chesapeake Bay impact structure as one of the largest and best preserved of the known impact craters on Earth, the ICDP and the USGS funded drilling of the central basin moat of the Chesapeake Bay impact structure in 2005–2006 on the Eyreville Farm, Cheriton, Virginia. Major objectives of the drilling include studies of: (1) processes directly related to impact, including crater excavation, crater collapse, late-stage infilling, and geometry of the resulting crater; (2) hydrogeologic changes, including determination of salinity and other chemical attributes of groundwater, which affect several million people in the area; (3) the deep biosphere, and the effects of impact on microbial activity; and (4) postimpact processes, which are the subject of this and two other companion papers in this volume (lithostratigraphy—Edwards *et al.*, this volume; regional correlations—Kulpecz *et al.*, this volume).

The Chesapeake Bay impact structure is located on a typical passive continental margin (“Atlantic-type”). Such margins typically feature quiescent tectonism and accommodation changes dominated by simple thermal subsidence, loading, compaction, and sea-level changes (e.g., Watts and Steckler, 1979; Kominz *et al.*, 1998). The postimpact strata offer the opportunity to investigate several unique characteristics that advance our understanding of the roles of sea-level, climate, and sediment-supply

changes on passive-margin stratigraphic records. Drilling the postimpact section in the central crater complements drilling to the north in New Jersey and Delaware as part of the Coastal Plain Drilling Project (Ocean Drilling Program [ODP] Legs 150X and 174AX; Miller et al., 2003a, 2006). This paper builds on the lithostratigraphic framework established by the onsite party and subsequent studies (Edwards et al., this volume) and provides the data for time correlations to New Jersey and Delaware (this paper), regional correlations (Kulpecz et al., this volume), and future studies that will quantify the effects of thermal subsidence, loading, and compaction ("backstripping"; e.g., Kominz et al., 1998) as has been done for core holes in the annular trough of

the Chesapeake Bay impact structure (Hayden et al., 2008). We do not make comparisons with core holes in the region (Exmore, Kiptopeke, Langley), which are considered in the context of regional tectonics by Kulpecz et al. (this volume).

METHODS

Core Hole Information

Eyreville coring ($37^{\circ}19'16.81''\text{N}$, $75^{\circ}58'31.89''\text{W}$; elevation 8 ft; Northampton County, Virginia, USGS 7.5 min quadrangle) began September 2005, recovering postimpact sediments from

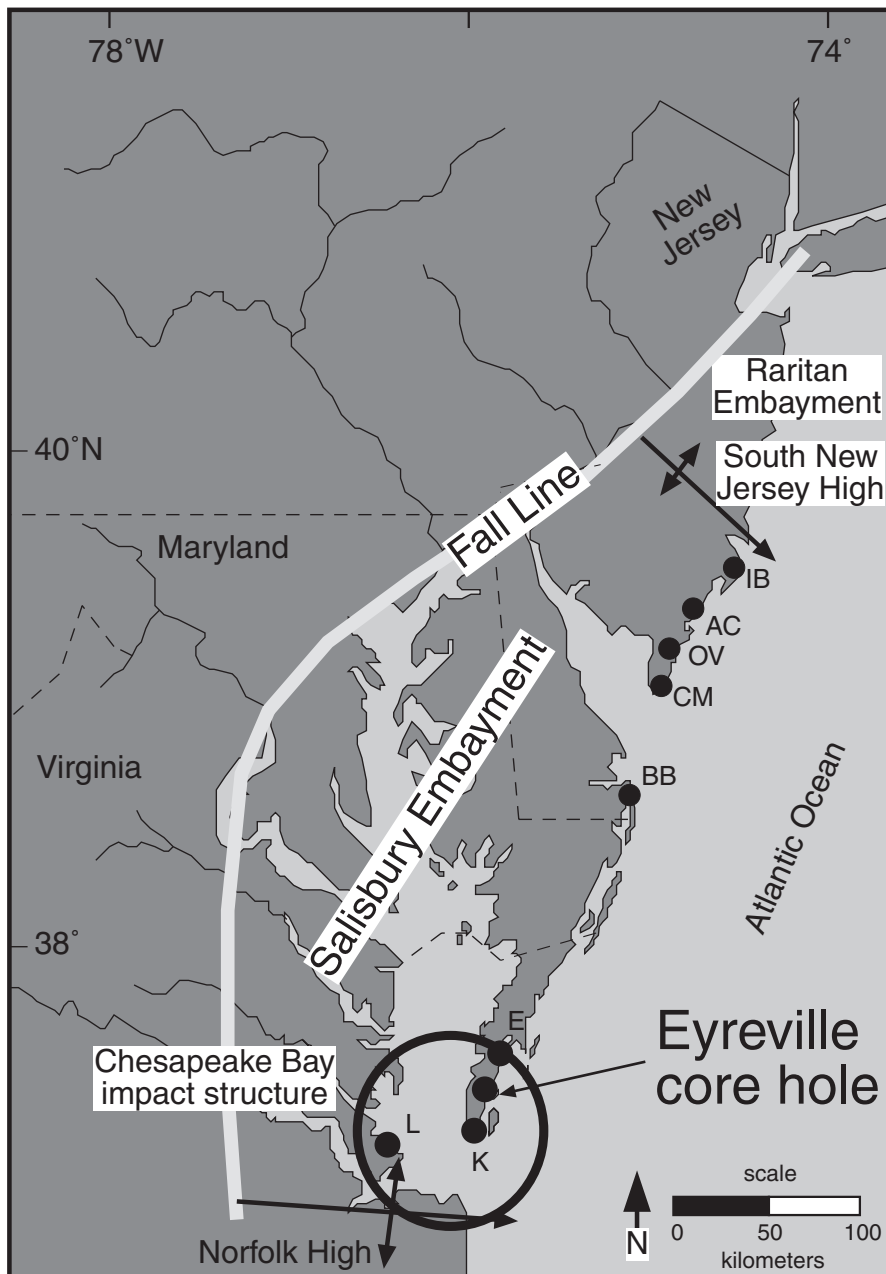


Figure 1. Location map showing the core holes drilled as a part of the New Jersey–Mid-Atlantic (MAT) sea-level transect and the Eyreville core hole. IB—Island Beach core hole; AC—Atlantic City core hole; CM—Cape May core hole; OV—Ocean View core hole; BB—Bethany Beach core hole; L—Langley core hole; K—Kiptopeke core hole; E—Exmore core hole.

the continuously cored Eyreville A core from 126.89 m to the top of the impactites at 443.88 m. The Eyreville C core was drilled within 10 m of core A in April–May 2006 from land surface to 139.57 m, overlapping the section cored in core A. The drill rods for core A were PQ with a core diameter of 8.4 cm, with a rock shoe and 7.6 cm with an extended shoe; HQ rods were used to drill core C with a core diameter of 6.1 cm with a rock shoe and 5.3 cm with a snout shoe. Recovery was excellent from the postimpact section of core A (95.9% recovered) and good from core C (69.1%), recovery from which was hampered by coarser-grained facies. A full suite of geophysical logs was obtained from core C, but only gamma logs and temperature logs through the rods were obtained from core A due to hole-stability problems.

Analysis of Core Material

The on-site scientific team provided preliminary descriptions of sedimentary textures, structures, colors, fossil content, identification of lithostratigraphic units (after Powars and Bruce, 1999), and lithologic contacts. These descriptions, including core recovery, lithologic descriptions, and assignment to local formations are discussed by Edwards et al. (this volume). Here, we integrate these lithologic descriptions with quantitative lithologic data, biostratigraphy, biofacies studies, Sr isotopic stratigraphy, and gamma logs. Our fundamental units are unconformity-bounded sequences, identified on the basis of physical stratigraphy, including irregular contacts, reworking, bioturbation, major facies changes, gamma-ray peaks, and paraconformities inferred from biostratigraphic and Sr isotopic breaks (Figs. 2–7). Cumulative percent of lithologic components of the sediments in the cores was computed from samples washed at ~1.52 m intervals for paleontological analysis (Table 1). Each sample was dried and weighed before washing, and the dry weight was used to compute the percentage of sand versus silt and clay (Table 1). The sand fraction was dry sieved through a 250 μm sieve, and the fractions were weighed to obtain a quantitative measure of the percent of very fine and fine versus medium and coarser sand. The sand fractions were examined using a microscope and a visual semiquantitative estimate was made of the relative percentages of quartz, glauconite, carbonate (foraminifers and other shells), mica, and other materials contained in the sample.

Biostratigraphy and Chronostratigraphy

Samples were examined for planktonic foraminiferal biostratigraphy at 1.52 m intervals and for dinocyst biostratigraphy at ~8 m intervals between 344.40 and 208.31 revised meters composite depth (rmcd). Nannofossils were examined for the Eocene section only (see Chronology section).

Sr isotopic age estimates (Table 2; Figs. 2–9) were obtained from mollusk and foraminifer shells (~4–6 mg) at the Eyreville borehole. Shells and foraminifer tests were cleaned ultrasonically and dissolved in 1.5 *N* HCl. Sr was separated using standard ion exchange techniques (Hart and Brooks, 1974). The

samples were analyzed on an Isoprobe T multicollector thermal ionization mass spectrometer (TIMS). Internal precision on the Isoprobe for the data set averaged ± 0.000010 and the external precision is approximately ± 0.000008 (based on replicate analyses of standards). NBS 987 was measured for these analyses at 0.710241 normalized to $^{86}\text{Sr}/^{88}\text{Sr}$ of 0.1194. Ages were assigned using the time scale of Berggren et al. (1995); the Miocene regressions of Oslick et al. (1994) were used where possible. The regressions given by Oslick et al. (1994) are only valid to sections older than 9.9 Ma (Sr isotopic values < 0.708930). Age errors for the late Miocene to early Pliocene vary, but they are generally quite large (> 1 Ma) in the early Pliocene due to a low rate of change (Martin et al., 1999). For the Pleistocene analysis, we derived a linear regression using the data of Farrell et al. (1995), correcting their data to NBS987 of 0.710255 and fitting a linear segment to the data between 0 and 2.5 Ma: Age = $15,235.08636 - 21,482.27712 \times (^{86}\text{Sr}/^{87}\text{Sr})$. For the Pliocene and late Miocene analyses, we used the ages obtained from the look-up tables of McArthur et al. (2001).

Miller et al. (1991) and Oslick et al. (1994) estimated age errors derived from linear regressions of Sr isotopic records. Age errors for 15.5–22.8 Ma are ± 0.61 Ma and 15.5–9.7 Ma are ± 1.17 Ma at the 95% confidence interval for a single analysis. Increasing the number of analyses at a given level improves the age estimate (± 0.40 and ± 0.76 Ma for three analyses each in the two intervals; Oslick et al., 1994). The regression for the late Pliocene–Pleistocene (0–2.5 Ma) has an age error of ± 0.35 Ma for one analysis at the 95% confidence interval to ± 0.2 Ma for three analyses at the 95% confidence interval (Miller, unpublished analysis of data of Farrell et al., 1995).

INTERPRETIVE FRAMEWORK OF SEQUENCES FROM THE MIDDLE ATLANTIC COASTAL PLAIN

The top portion of the Eyreville core hole (< 249.94 m) generally displays classic, repetitive transgressive-regressive facies changes within sequences (Owens and Sohl, 1969; Sugarman et al., 1993, 1995) that consist of: (1) a basal, generally thin, transgressive quartz sand equivalent to the transgressive systems tract (TST) of Posamentier et al. (1988); and (2) a coarsening-upward succession of medial regressive silt and upper quartz sand equivalent to the highstand systems tract (HST) of Posamentier et al. (1988). Lowstand systems tracts (LSTs) were not identified in the Eyreville cores, as is typical for updip sections in the mid-Atlantic coastal plain (Browning et al., 2008). When TSTs are thin, maximum flooding surfaces (MFS) are difficult to differentiate from unconformities because shell beds and gamma-ray peaks mark both. Flooding surfaces (FS), particularly MFSs, may be differentiated from sequence boundaries by the association of erosion and rip-up clasts at the latter, lithofacies successions, and benthic foraminiferal changes. The transgressive surface (TS), marking the top of the LST, represents a change from generally regressive to transgressive facies; because LSTs are absent, these surfaces are merged with sequence boundaries. The postimpact section

TABLE 1. SUMMARY OF SEDIMENT COMPONENTS IN SAMPLES FROM THE POSTIMPACT SECTION OF THE EYREVILLE A
AND C CORE HOLES

Eyreville core C								
Sample depth (rmcd)	Sample depth (ft)	% Clay & silt	% Glauconite*	% Fine quartz sand*	% Medium quartz sand*	% Carbonate*	% Mica*	% Other*
1.83	6.0	11.4	0	81	8	0	0	0
3.44	11.3	8.0	0	44	48	0	0	0
4.85	15.9	0.9	0	51	48	0	0	0
6.40	21.0	5.4	0	52	42	0	0	0
7.99	26.2	14.3	0	68	17	0	1	1
9.45	31.0	91.7	0	2	0	5	1	0
10.97	36.0	15.2	0	76	0	4	3	2
12.53	41.1	66.0	0	28	0	3	2	1
13.93	45.7	12.0	0	82	1	0	3	3
17.07	56.0	9.6	0	39	31	4	2	14
18.68	61.3	11.2	3	40	27	19	0	0
20.12	66.0	8.2	4	44	21	23	0	0
21.64	71.0	22.5	3	38	16	19	0	0
23.16	76.0	20.1	4	43	14	19	0	0
25.15	82.5	19.2	1	46	16	17	0	0
26.37	86.5	21.5	1	50	10	16	0	0
28.41	93.2	26.9	1	50	7	15	0	0
29.02	95.2	29.6	0	44	4	23	0	0
30.78	101.0	38.0	0	37	4	20	0	0
33.99	111.5	27.9	3	26	29	13	0	0
36.88	121.0	28.4	1	46	15	9	0	0
38.40	126.0	24.4	11	27	34	4	0	0
39.99	131.2	13.2	3	58	22	4	0	0
41.42	136.0	10.2	7	60	23	0	0	0
43.25	141.9	10.2	1	79	10	0	0	0
44.50	146.0	11.3	0	77	4	8	0	0
46.02	151.0	8.6	0	76	6	9	0	1
47.52	155.9	10.6	1	60	8	20	0	1
49.13	161.2	13.7	1	49	34	2	0	0
50.60	166.0	18.1	4	43	32	2	0	0
52.12	171.0	27.0	6	26	40	1	0	0
53.64	176.0	36.0	5	29	28	1	0	0
55.17	181.0	19.1	5	26	50	0	0	0
56.62	186.0	79.9	1	16	0	0	2	1
58.22	191.0	34.5	33	11	22	0	0	0
59.22	194.3	18.9	21	27	12	21	0	0
61.48	201.7	14.0	15	37	34	0	0	0
62.79	206.0	11.0	3	46	40	0	0	0
64.40	211.3	14.4	4	49	12	20	0	0
65.84	216.0	9.0	4	62	9	16	0	0
67.36	221.0	10.8	1	75	6	6	0	1
69.22	227.1	12.5	0	78	2	8	0	0
70.50	231.3	24.6	0	61	1	13	0	0
71.93	236.0	7.5	1	65	25	1	0	0
73.67	241.7	51.9	1	45	0	2	0	0
74.98	246.0	52.6	1	41	0	5	1	0
76.50	251.0	58.8	1	38	0	2	1	0
79.64	261.3	37.2	1	56	3	1	1	0
81.08	266.0	40.0	6	44	8	0	1	1
88.70	291.0	7.7	0	86	6	1	0	0
90.22	296.0	6.9	0	23	23	47	0	0
91.74	301.0	5.0	0	87	3	3	2	0
93.27	306.0	3.6	0	82	3	12	0	0
94.79	311.0	7.1	0	92	1	1	0	0
95.71	314.0	37.1	0	63	0	0	0	0
101.10	331.7	14.0	2	83	0	1	0	0
102.41	336.0	13.2	0	87	0	0	0	0
103.97	341.1	14.4	2	74	7	4	0	0
105.55	346.3	17.0	2	80	1	0	0	0
108.72	356.7	20.1	3	70	5	1	0	0
110.19	361.5	11.6	0	88	0	0	0	0
111.56	366.0	19.7	0	79	0	0	2	0
113.08	371.0	17.4	0	82	0	0	0	0
113.20	371.4	24.2	0	75	0	0	1	0
113.85	374.3	23.3	0	76	0	0	1	0
116.16	381.1	25.6	0	73	0	0	1	0
117.65	386.0	23.5	0	54	0	21	2	0
119.33	391.5	36.3	0	59	0	4	0	0
120.40	395.0	43.3	0	53	0	4	0	0
122.22	401.0	74.1	0	25	0	1	0	0
124.15	407.3	57.3	0	39	0	3	0	0
125.70	412.4	50.5	0	48	0	1	1	0

(Continued)

TABLE 1. SUMMARY OF SEDIMENT COMPONENTS IN SAMPLES FROM THE POSTIMPACT SECTION OF THE EYREVILLE A
AND C CORE HOLES (Continued)

Eyreville A core								
Sample depth (rmcd)	Sample depth (ft)	% Clay & silt	% Glauconite*	% Fine quartz sand*	% Medium quartz sand*	% Carbonate*	% Mica*	% Other*
127.47	418.2	74.5	0	25	0	0	1	0
128.99	423.2	89.1	0	10	0	0	0	0
129.88	426.1	95.7	0	4	0	0	0	0
131.28	430.7	93.9	0	5	0	1	0	0
132.28	434.0	93.6	0	5	0	1	0	1
134.63	441.7	90.4	0	3	0	3	1	3
135.85	445.7	79.2	0	19	0	0	1	0
137.50	451.1	65.1	0	33	0	0	1	0
139.84	458.8	81.7	0	16	0	1	1	0
140.54	461.1	94.6	0	5	0	0	0	0
142.04	466.0	98.9	0	1	0	0	0	0
143.56	471.0	99.1	0	1	0	0	0	0
145.02	475.8	99.0	0	1	0	0	0	0
146.55	480.8	99.0	0	0	0	0	0	0
147.88	485.18	99.0	0	0	0	0	0	0
149.66	491.0	91.7	0	6	0	0	0	1
151.19	496.1	95.2	0	2	0	2	0	0
152.68	501.0	92.1	0	4	0	4	0	0
154.20	506.0	81.4	0	17	0	1	0	0
155.75	511.0	96.9	0	3	0	0	0	0
157.23	516.0	61.3	0	36	0	1	0	0
158.77	520.9	50.1	0	47	0	1	0	0
160.23	526.0	67.9	0	31	0	0	1	0
161.85	531.0	89.3	0	10	0	0	0	0
163.33	536.2	95.9	0	4	0	0	0	0
164.71	540.5	89.3	0	10	0	0	0	0
166.35	546.0	95.3	0	4	0	0	0	0
167.94	551.0	99.4	0	0	0	0	0	0
169.40	556.0	99.6	0	0	0	0	0	0
171.27	561.9	99.1	0	0	0	0	0	0
172.49	565.9	98.2	0	0	0	0	0	1
175.60	571.1	99.5	0	0	0	0	0	0
177.09	576.0	99.9	0	0	0	0	0	0
178.31	580.0	99.7	0	0	0	0	0	0
180.01	585.6	97.1	0	2	0	0	0	0
181.51	591.0	91.5	0	8	0	0	0	0
183.03	596.0	86.7	0	13	0	0	0	0
184.59	601.1	94.0	0	5	0	0	0	0
187.49	610.3	96.6	0	3	0	0	0	0
189.27	616.2	92.5	0	7	0	0	0	0
190.46	620.3	93.9	0	6	0	0	0	0
192.31	626.2	95.7	0	4	0	0	0	0
193.48	630.3	98.2	0	2	0	0	0	0
196.05	638.2	99.5	0	0	0	0	0	0
196.69	640.3	99.5	0	0	0	0	0	0
198.33	645.7	98.1	0	2	0	0	0	0
201.18	655.5	96.5	0	3	0	0	0	0
203.21	661.7	98.6	0	1	0	0	0	0
204.43	665.7	98.8	0	0	0	1	0	0
205.01	667.6	99.2	0	0	0	0	0	0
206.13	671.6	94.0	0	4	0	0	0	2
209.25	681.6	75.4	0	23	0	0	1	0
209.28	681.7	70.0	0	28	0	0	1	0
210.26	685.1	84.2	0	14	0	0	1	1
210.51	686.0	91.2	0	8	0	0	0	0
213.66	696.0	94.1	0	5	0	0	0	0
215.22	701.1	97.9	0	1	0	1	0	0
216.74	706.1	98.2	0	1	0	1	0	0
218.27	711.1	98.7	0	0	0	1	0	0
219.76	716.0	94.0	0	5	0	0	0	0
221.28	721.0	80.1	1	18	0	0	1	0
224.47	736.46	76.8	1	21	0	0	1	0
227.27	746.45	86.1	0	12	0	0	1	0
227.28	746.46	84.0	0	0	0	0	0	0
228.80	751.46	82.4	0	16	0	0	1	0
230.42	756.0	91.5	0	8	0	0	0	0
232.06	761.5	94.3	0	5	0	0	0	0
233.43	765.84	97.4	0	2	0	0	0	0
235.21	771.7	91.1	0	8	0	1	0	0

(Continued)

TABLE 1. SUMMARY OF SEDIMENT COMPONENTS IN SAMPLES FROM THE POSTIMPACT SECTION OF THE EYREVILLE A AND C CORE HOLES (Continued)

Eyreville A core								
Sample depth (rmcd)	Sample depth (ft)	% Clay & silt	% Glauconite*	% Fine quartz sand*	% Medium quartz sand*	% Carbonate*	% Mica*	% Other*
236.69	776.84	98.9	0	1	0	0	0	0
238.21	781.84	98.5	0	1	0	0	0	0
239.54	785.9	95.0	0	5	0	0	0	0
241.16	791.2	99.0	0	0	0	1	0	0
242.66	796.2	99.2	0	0	0	1	0	0
244.19	801.4	97.5	0	1	0	1	0	0
245.88	806.7	98.3	0	0	0	1	0	0
247.22	811.1	97.6	0	1	0	1	0	0
248.87	816.5	67.1	0	26	0	7	0	0
250.30	821.2	76.9	0	18	0	5	0	0
251.93	826.6	93.3	0	5	0	2	0	0
253.28	831.12	86.5	0	11	0	3	0	0
254.72	836.0	89.8	0	9	0	2	0	0
256.04	840.9	75.8	0	23	0	1	0	0
257.79	846.0	88.0	0	11	0	1	0	0
259.33	851.4	96.5	0	1	0	2	0	0
261.00	856.5	94.2	0	4	0	2	0	0
261.03	856.6	94.6	0	3	0	2	0	0
262.31	861.0	97.5	0	0	0	2	0	0
263.84	865.7	99.2	0	0	0	1	0	0
265.41	871.0	99.9	0	0	0	0	0	0
267.11	876.6	99.3	0	0	0	0	0	0
268.46	881.3	98.8	0	0	0	1	0	0
269.93	885.9	99.7	0	0	0	0	0	0
269.96	886.0	99.4	0	0	0	0	0	0
271.37	891.0	99.2	0	0	0	0	0	0
273.11	896.3	98.7	0	1	0	1	0	0
274.46	901.0	99.7	0	0	0	0	0	0
276.23	906.4	89.9	0	0	0	10	0	0
277.53	910.8	99.1	0	0	0	1	0	0
279.14	915.8	98.5	0	0	0	2	0	0
280.84	921.4	98.3	0	0	0	1	0	0
282.21	926.2	98.7	0	0	0	1	0	0
283.64	931.2	93.3	0	1	0	6	0	0
283.89	931.4	97.2	0	1	0	2	0	0
285.33	936.4	96.9	0	1	0	2	0	0
286.74	941.3	99.4	0	0	0	1	0	0
288.52	946.6	99.5	0	0	0	1	0	0
290.04	951.6	98.8	0	0	0	1	0	0
291.37	956.4	98.3	0	0	0	2	0	0
291.40	956.5	98.2	0	0	0	2	0	0
293.13	961.74	97.8	0	0	0	2	0	0
294.61	966.74	98.1	0	0	0	2	0	0
296.19	971.74	95.4	0	0	0	5	0	0
297.71	976.74	94.8	0	0	0	5	0	0
299.01	981.0	92.4	0	0	0	7	0	0
300.76	986.74	95.7	0	0	0	4	0	0
302.28	991.74	88.2	0	0	0	12	0	0
303.81	996.74	96.2	0	0	0	4	0	0
304.99	1001.12	97.8	0	0	0	2	0	0
306.51	1006.12	97.5	0	0	0	2	0	0
308.17	1011.12	96.7	0	0	0	3	0	0
309.63	1016.12	99.0	0	0	0	1	0	0
311.24	1021.12	98.7	0	0	0	1	0	0
312.76	1026.11	94.0	0	0	0	6	0	0
314.29	1031.12	98.7	0	0	0	1	0	0
315.81	1036.11	96.3	0	0	0	4	0	0
317.42	1041.5	97.2	0	0	0	3	0	0
318.87	1046.5	98.2	0	0	0	2	0	0
320.47	1051.4	98.4	0	0	0	2	0	0
322.02	1056.5	98.5	0	0	0	1	0	0
324.73	1065.4	86.4	0	0	0	14	0	0
324.76	1065.5	98.3	0	0	0	2	0	0
326.56	1071.4	95.7	0	0	0	4	0	0
326.71	1071.88	80.1	0	0	0	20	0	0
328.12	1076.5	91.4	0	0	0	9	0	0
329.61	1081.88	81.3	0	0	0	19	0	0
331.08	1086.78	92.4	0	0	0	8	0	0
334.23	1096.87	78.6	0	0	0	21	0	0

(Continued)

TABLE 1. SUMMARY OF SEDIMENT COMPONENTS IN SAMPLES FROM THE POSTIMPACT SECTION OF THE EYREVILLE A
AND C CORE HOLES (Continued)

Sample depth (rmcd)	Sample depth (ft)	% Clay & silt	Eyreville A core					% Other*
			% Glauconite*	% Fine quartz sand*	% Medium quartz sand*	% Carbonate*	% Mica*	
335.84	1101.88	90.7	0	0	0	9	0	0
337.30	1106.78	84.3	0	0	0	15	0	0
338.87	1111.78	98.6	0	0	0	1	0	0
340.42	1116.87	94.0	0	0	0	6	0	0
341.10	1119.1	98.0	0	0	0	2	0	0
341.76	1121.26	99.1	0	0	0	1	0	0
342.03	1122.16	99.0	0	0	0	1	0	0
342.63	1124.1	98.7	0	0	0	1	0	0
343.20	1126.0	96.3	0	0	0	3	0	0
343.25	1126.16	93.5	0	0	0	6	0	0
343.78	1127.9	83.6	4	0	0	9	0	4
344.08	1128.9	52.2	12	0	0	24	0	12
344.55	1130.5	39.6	32	1	1	2	0	25
344.90	1131.7	77.7	15	0	0	0	0	7
345.62	1134.16	59.1	9	20	0	0	0	12
346.21	1136.16	43.3	19	28	0	0	0	10
346.94	1138.26	43.6	13	12	0	13	0	19
347.03	1138.55	85.8	0	0	0	13	0	0
347.53	1140.2	44.7	15	15	0	23	0	2
348.17	1142.3	90.7	1	1	0	7	0	0
348.45	1143.2	89.1	1	1	0	9	0	0
348.55	1143.55	84.3	3	6	0	6	0	0
349.18	1145.6	36.2	19	19	0	26	0	0
349.82	1147.7	34.1	35	24	0	7	0	0
350.49	1150.0	99.4	0	0	0	0	0	0
350.86	1151.3	99.5	0	0	0	0	0	0
352.29	1156.3	99.2	0	0	0	0	0	0
353.99	1161.54	94.0	3	0	0	3	0	0
354.02	1161.64	94.9	2	0	0	2	0	0
355.49	1166.64	98.5	0	0	0	1	0	0
356.93	1171.04	98.6	0	0	0	1	0	0
358.49	1176.14	97.8	0	0	0	2	0	0
360.13	1181.54	96.6	0	0	0	3	0	0
361.59	1186.54	96.9	0	0	0	3	0	0
362.95	1191.44	97.4	0	0	0	2	0	0
364.64	1196.42	97.4	0	0	0	3	0	0
366.12	1201.42	98.0	0	0	0	2	0	0
367.55	1206.0	97.9	0	0	0	2	0	0
368.96	1211.0	96.0	0	0	0	4	0	0
370.33	1215.0	99.0	0	0	0	1	0	0
372.16	1221.0	96.7	0	0	0	3	0	0
373.53	1225.5	96.7	0	1	0	2	0	0
381.30	1251.0	97.1	0	1	0	1	0	0
382.83	1256.0	95.2	2	2	0	1	0	0
384.35	1261.0	98.3	0	0	0	1	0	0
385.88	1266.0	96.3	1	1	0	1	0	0
387.55	1271.5	97.0	0	0	0	3	0	0
388.92	1276.0	98.4	0	0	0	1	0	0
395.17	1296.6	97.7	0	0	0	2	0	0
396.53	1301.0	97.5	0	0	0	2	0	0
398.22	1306.5	97.1	0	0	0	1	0	1
399.38	1310.3	98.7	0	0	0	0	0	1
400.72	1316.7	98.4	0	0	0	0	0	1
402.00	1321.0	98.4	0	0	0	0	0	1
404.16	1326.0	98.4	0	0	0	0	0	1
405.94	1334.6	97.2	0	0	0	0	0	2
406.43	1336.25	98.6	0	0	0	0	0	1
407.85	1341.0	98.5	0	0	0	0	0	1
410.26	1346.0	98.7	0	0	0	0	0	1
413.34	1356.9	98.6	0	0	0	0	0	1
414.59	1361.0	99.0	0	0	0	0	0	1
416.36	1366.0	99.3	0	0	0	1	0	0
419.22	1376.0	99.7	0	0	0	0	0	0
420.75	1381.0	99.8	0	0	0	0	0	0
422.45	1386.0	99.8	0	0	0	0	0	0
423.98	1391.0	99.8	0	0	0	0	0	0
425.43	1396.0	99.6	0	0	0	0	0	0
426.85	1401.0	99.9	0	0	0	0	0	0
428.53	1406.0	99.6	0	0	0	0	0	0
430.03	1411.0	99.9	0	0	0	0	0	0

(Continued)

TABLE 1. SUMMARY OF SEDIMENT COMPONENTS IN SAMPLES FROM THE POSTIMPACT SECTION OF THE EYREVILLE A AND C CORE HOLES (Continued)

Eyreville A core							
Sample depth (rmcd)	Sample depth (ft)	% Clay & silt	% Glauconite*	% Fine quartz sand*	% Medium quartz sand*	% Carbonate*	% Other*
431.60	1416.0	99.9	0	0	0	0	0
434.64	1426.0	99.9	0	0	0	0	0
436.18	1431.1	99.9	0	0	0	0	0
437.69	1436.0	98.1	0	0	0	2	0
440.27	1446.05	99.9	0	0	0	0	0

*Obtained by visual best estimate; see "Methods." These data were used to construct cumulative percent plots on Figures 2–9. Note that the percent silt and clay in each sample was quantitatively measured by weighing each sample before and after washing off the clay and silt. All other percentages were arrived at qualitatively by visually estimating the proportion of each constituent in the sand fraction. Errors for the visual estimates are $\pm 5\%$.

rmcd—revised meters composite depth.

TABLE 2. STRONTIUM ISOTOPIC RATIOS AND AGE ESTIMATES FROM THE EYREVILLE A AND C CORE HOLES

Eyreville core C						
Sample depth (rmcd)	Sample depth (ft)	Material	Sr value	Error	Age (Ma)	McArthur age (Ma)
7.25	23.8	Shell	0.709165	0.000014	0.35	
9.83	32.25	Shell	0.709170	0.000008	0.24	
10.64	34.9		0.709147	0.000008	0.74	
16.28	53.4	Shell	0.709162	0.000007	0.41	
20.48	67.2		0.709058	0.000007	5.2	2.8
21.64	71.0	Shell	DNR			
21.79	71.5		0.709072	0.000008	5.0	2.3
23.65	77.6		0.709057	0.000008	5.2	2.9
25.85	84.8		0.709066	0.000006	5.1	2.5
26.37	86.5	Shell	0.709850	0.000009	–14.4	
28.77	94.4		0.709038	0.000008	5.5	4.7
31.67	103.9		0.709036	0.000008	5.5	4.8
33.99	111.5	Shell	0.709043	0.000006	5.4	4.5
34.15	112.1		DNR			
38.40	126.0	Shell	0.709060	0.000011	5.1	2.7
39.75	130.4	Shell	DNR			
39.75	130.4R	Shell	0.709091	0.000045	1.9	1.6
42.03	138		0.709082	0.000008	2.1	2.0
42.31	138.9	Shell	0.709059	0.000007	5.2	2.8
43.40	142.4	Shell	0.709035	0.000007	5.5	4.9
45.08	147.9	Shell	0.708967	0.000011	6.5	6.4
45.93	150.7	Shell	0.709005	0.000021	6.0	5.7
46.92	153.95		0.709037	0.000011	5.5	4.8
47.55	156.0	Shell	0.709046	0.000008	5.4	4.2
48.28	158.4	Shell	0.709008	0.000010	5.9	5.7
50.60	166.0	Shell	0.709898	0.000008	–15.4	
51.85	170.1	Shell	0.709064	0.000008	5.1	2.5
54.04	177.3	Shell	0.709015	0.000006	5.8	5.5
54.10	177.5		0.709040	0.000008	5.4	4.7
55.47	182.0	Shell	DNR			
58.03	190.4	Shell	0.709016	0.000008	5.8	5.5
59.01	193.6	Shell	0.708968	0.000008	6.5	6.4
62.67	205.6	Shell	0.709005	0.000007	6.0	5.7
63.23	207.45	Shell	0.708984	0.000018	6.3	6.1
65.84	216.0	Shell	0.709030	0.000015	5.6	5.2
67.36	221.0	Shell	0.708961	0.000008	6.6	6.8
69.65	228.5	Shell	0.708947	0.000010	6.8	7.1
70.50	231.3	Shell	DNR			
71.87	235.8	Shell	0.708998	0.000007	6.1	5.8
74.98	246.0	Shell	0.708948	0.000005	6.8	7.1
76.60	251.3	Shell	0.708964	0.000009	6.6	6.5
85.54	280.7	Shell	0.708953	0.000013	6.8	6.9
90.13	295.7	Shell	0.708968	0.000006	6.5	6.4
90.19	295.9	Shell	0.708949	0.000008	6.8	7.0
106.77	350.3	Shell	0.708959	0.000008	6.7	6.7
115.39	379.6	Shell	0.708969	0.000007	6.5	6.4
120.40	395.0	Shell	0.708975	0.000009	6.4	6.2
123.57	405.4	Shell	0.708945	0.000007	6.9	7.2
135.94	446.0	Shell	0.708949	0.000007	6.8	7.0

(Continued)

TABLE 2. STRONTIUM ISOTOPIC RATIOS AND AGE ESTIMATES FROM THE EYREVILLE A AND C CORE HOLES (*Continued*)

Eyreville core A						
Sample depth (rmcd)	Sample depth (ft)	Material	Sr value	Error	Age (Ma)	McArthur age (Ma)
426.2	129.9	Shell	DNR			
426.2R	129.9	Shell	DNR			
426.2R	129.9	Shell	0.708958	0.000008	6.7	6.7
434.9	132.6	Shell	0.708958	0.000005	6.7	6.7
434.9R	132.6	Shell	0.708949	0.000025	6.8	7
465	141.7	Shell	0.708953	0.000004	6.8	6.9
496.1	151.2	Shell	0.709010	0.000013	5.9	5.6
496.1R	151.2	Shell	0.708937	0.000008	7.0	7.5
501.0	152.7	Shell	0.708974	0.000007	6.4	6.3
536.2	163.4	Shell	0.708970	0.000008	6.5	6.4
561.9	171.3	Shell/For	0.708960	0.000007	6.7	6.6
571.1	174.1	Forams	0.708951	0.000007	6.8	7
591.0	180.1	Shell	0.708940	0.000007	7.0	7.4
591.0	180.1	Forams	0.708941	0.000007	6.9	7.3
626.2	190.9	Forams	0.708936	0.000007	7.0	7.5
665.7	202.9	Forams	0.708595	0.000026	18.3	
701.1	213.7	Forams	0.708806	0.000007	14.1	
706.1	215.2	Forams	0.708835	0.000006	12.3	
711.1	216.7	Forams	DNR			
716.0	218.2	Forams	0.708861	0.000008	11.5	
771.7	235.2	Forams	0.708887	0.000016	10.7	
791.2	241.2	Forams	0.708842	0.000008	12.1	
826.6	251.9	Shell	0.708839	0.000021	12.1	
861.0	262.4	Forams	0.708818	0.000008	13.7	
910.8	277.6	Shell	0.708847	0.000008	11.9	
956.4	291.5	Shell	DNR			
1001.1	305.1	Forams	DNR			
1001.1	305.14	Shell	0.708797	0.000008	14.5	
1026.1	312.76	Forams	0.708739	0.000005	16.2	
1046.5	318.97	Forams	0.708685	0.000013	17.0	
1051.4	320.47	Forams	0.708791	0.000016	14.7	
1056.5	322.02	Forams	0.708808	0.000016	14.1	
1065.4	324.7	Forams	0.708731	0.000006	16.3	
1071.88	326.71	Shell	0.708650	0.000008	17.5	
1076.5	328.1	Forams	0.708745	0.000005	16.1	
1081.9	329.8	Forams	0.708727	0.000008	16.3	
1086.8	331.3	Forams	0.708680	0.000008	17.0	
1096.9	334.3	Shell	0.708649	0.000015	17.5	
1096.9	334.3	Forams	0.708682	0.000015	17.0	
1106.78	337.3	Shell	0.708718	0.000014	16.5	
1111.8	338.9	Forams	0.708585	0.000016	18.4	
1116.7	340.4	Forams	0.708587	0.000006	18.4	
1121.3	341.8	Forams	0.708608	0.000009	18.1	
1126.0	343.2	Forams	0.708774	0.000007	15.6	
1128.9	344.1	Forams	0.708605	0.000010	18.1	
1138.16	346.9	Forams	0.708232	0.000008	24.4	
1138.55	347.0	Forams	0.708092	0.000007	27.2	
1140.2	347.5	Forams	0.708119	0.000006	26.6	
1143.2	348.4	Forams	DNR			
1145.6	349.2	Forams	0.708074	0.000008	27.7	
1161.64	354.1	Forams	DNR			

Note: rmcd—revised meters composite depth; DNR—did not run.

at Eyreville generally fines downsection, and sand is virtually absent from ~249.94 to 344.73 and from 349.91 to 441.96 m. As a result, the lithologic signature of sequences in these intervals is very subdued.

The overall association of facies suggests that most of the Eyreville section fits a wave-dominated shoreline model devised by Bernard et al. (1962) on Galveston Island and further devel-

oped by Harms et al. (1975, 1982), and McCubbin (1982). The facies model used in this study has been detailed by Browning et al. (2008) and recognizes the following environments (Fig. 2):

(1) Fluvial to upper estuarine: dominantly sand, including likely cut-and-fill channels lined with gravels mostly composed of clean sands with little clay; sands generally poorly sorted; commonly lignitic.

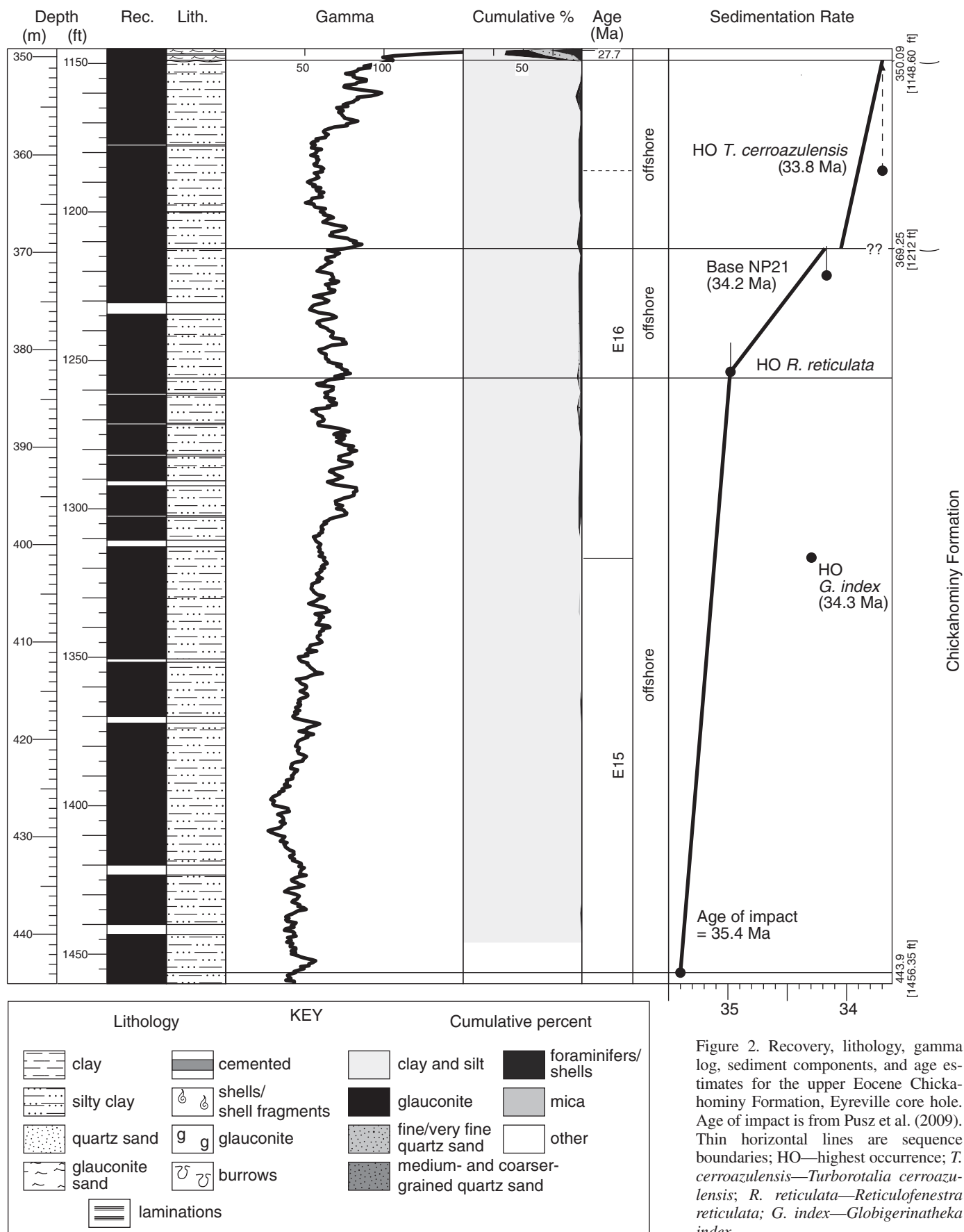


Figure 2. Recovery, lithology, gamma log, sediment components, and age estimates for the upper Eocene Chickahominy Formation, Eyreville core hole. Age of impact is from Pusz et al. (2009). Thin horizontal lines are sequence boundaries; HO—highest occurrence; *T. cerroazulensis*—*Turborotalia cerroazulensis*; *R. reticulata*—*Reticulofenestra reticulata*; *G. index*—*Globigerinatheka index*.

(2) Lower estuarine: poorly sorted sands admixed with inter-laminated thin sands and clays; commonly lignitic, commonly associated with “beachy” sands.

(3) Upper shoreface/foreshore: clean “beachy” sands of fine to coarse admixtures, with opaque heavy mineral laminae highlighting cross-bedding; most probably upper shoreface, since foreshore deposits are less commonly preserved.

(4) Distal upper shoreface: fine to medium sands, clean in places, others with admixed silts and scarce clay layers; usually showing evidence of heavy bioturbation that tends to obscure lamination.

(5) Lower shoreface: interbedded fine and very fine sands, generally silty due to mixing, and commonly very shelly with whole shells preserved; deposited below fair-weather wave base but within storm wave base.

(6) Offshore: thinly laminated very fine sands, silts, and clays; deposited below storm wave base, with finer sediments representing deposition further offshore. Changes in water depth are difficult to determine using lithology but an increased percentage of carbonate in the sand fraction is inferred to represent deeper-water deposition.

SEQUENCE STRATIGRAPHY

Eocene Sequences

Eocene sediments consist primarily of clays assigned to the Chickahominy Formation (Edwards et al., this volume) that were deposited in deep water (~300 m, Poag, this volume; ~200 m, this study). The Eocene section is relatively homogeneous and resists sequence stratigraphic subdivision, but it is tentatively divided into two sequences (see also Schulte et al., this volume).

The base of the Chickahominy Formation (443.90–350.09 rmcd) is at 443.90 rmcd, where there is very sharp contact with the underlying impact breccia. Typical Exmore beds breccias, found below 444.34 rmcd, consist of a matrix of glauconitic, granular fine to very coarse, cross-bedded to massive quartz sand with clasts of clay, igneous, and metamorphic rocks to 13 mm diameter. A transition zone at the top of the Exmore beds extends from 444.34 to 443.90 rmcd and consists of finely laminated, wavy clay that fines upsection (Poag, this volume). The Chickahominy Formation in the Eyreville core hole (Fig. 2; Table 3) is remarkably uniform silty clay to clayey silt and contains scattered pyrite, scattered foraminifers and mollusk shells, and rare mica and glauconite (<1%–2%) (see also Schulte et al. [this volume] for an expanded discussion of the Chickahominy Formation lithofacies). The formation is generally heavily bioturbated and structureless but locally contains faint laminations. There are no obvious surfaces or facies changes in the uniform section, making sequence stratigraphic subdivision difficult. The entire section is late Eocene, and there is no faunal or floral evidence for Oligocene strata. This constrains the section to 35.4 Ma (i.e., the estimated time of the impact; Pusz et al., 2009) to 33.7 Ma using the time scale of Berggren et al. (1995) as

modified by Berggren and Pearson (2005). Other than this, age control based on biostratigraphy is limited (Fig. 2), though it is clear that the section was deposited at high rates (~50 m/Ma). A possible break in sedimentation rates at 369.25 rmcd is associated with a gamma log kick. This ca. 34 Ma contact may represent a subtle sequence boundary.

The Chickahominy Formation was deposited in deep outer neritic to upper bathyal environments (100–600 m). Based on the relatively high abundance (though not dominance) of agglutinated benthic foraminifers, Poag (this volume) interpreted the depositional environment as a high-stress and possibly low-oxygen basin. The remarkably uniform and fine-grained strata support the interpretation that the basin was restricted. The unique paleoecology of a restricted basin limits our paleodepth resolution. Still, we interpret that the section was deposited in the outer neritic to uppermost bathyal zones (~200 ± 100 m) based on a diverse assemblage of benthic foraminifers including of *Globobulimina*, *Cibicidoides*, *Bulimina jacksonensis*, *Siphonina*, and *Fronicularia*.

Very Condensed Oligocene Sequences

Oligocene sediments in the Eyreville core hole are glauconitic and contain several burrowed contacts (Fig. 3; Table 3). We divide the Oligocene into two sequences. The lower sequence (350.09–348.02 rmcd) corresponds to the Drummonds Corner beds (Edwards et al., this volume; see also Powars et al., 2005). The upper sequence (348.02–344.74 rmcd) corresponds to the lower part of the Old Church Formation (Edwards et al., this volume).

The contact between the Oligocene glauconite sand and the underlying Chickahominy Formation (350.09 rmcd) is sharp and burrowed. Glauconite filled burrows extend down to 355.90 rmcd, over 5.8 m below the contact. The base of the sequence (350.09–349.72 rmcd) consists of fine glauconite sand (~60% glauconite). From 349.72 rmcd to a contact at 348.72 rmcd, there is semi-indurated (349.73–349.48 rmcd) burrowed, muddy, quartzose (to 20%), very fine glauconite sand with common foraminifers, thin bivalve shells, and decreasing glauconite upsection. The contact at 348.72 rmcd separates more glauconitic sediment below from less glauconitic sediment above and is interpreted as the MFS. In the overlying HST, the section becomes less glauconitic upsection between 348.72 and 348.49 rmcd in a silty clay with abundant foraminifers (especially along partings). From 348.49 to 347.96 rmcd, the section is brownish green, silty clay in which foraminifers grow less common to a contact zone between 348.15 and 347.96 rmcd interpreted to be the upper sequence boundary. Based on Sr isotopes, the thin sequence from 350.09 to 347.96 rmcd sequence was deposited ca. 28 Ma (see Chronology section) and correlates with sequence O4 in New Jersey (Pekar et al., 2002).

A contact and transgressive lag interval from 348.14 to 347.96 rmcd contains blebs of material burrowed down into the darker, brownish green silty clay below (Fig. 3; Table 3). Above

the contact (347.96–347.14 rmcd), the sediments are heavily burrowed, slightly micaceous, clayey silt with very abundant foraminifers, and silty, very fine to coarse glauconite (3%–5%). The change to more glauconitic sediments above a burrowed contact is interpreted to represent a sequence boundary. Above 347.14–346.95 rmcd, the sediments are clayey, heavily bioturbated silt, and the change back to fine-grained, less glauconitic sediment is interpreted as the MFS. The section coarsens above the MFS to foraminifera-rich, sandy, micaceous, silt to 346.39 rmcd and to silty glauconitic, very fine sand to a burrowed surface at

345.61 rmcd, which is interpreted as a flooding surface. From 345.61 rmcd to the upper sequence boundary at 344.70 rmcd, the sediments are sandy silt that fines upward, with very fine glauconite and common foraminifers. The HST is apparently truncated and that may explain why the sequence fines toward the top. Based on lithology, these sediments were deposited in inner to middle neritic paleodepths. The thin sequence from 347.96 to 344.70 rmcd is approximately ca. 27 Ma in age (see Chronology section) and correlates with sequence O3 in New Jersey (Pekar et al., 2002).

TABLE 3. SEQUENCES IN THE EYREVILLE A AND C CORE HOLES

Sequence	Depth (ft)	Depth (m)	Age (Ma)	Error low (Ma)	Error high (Ma)	Hiatus (Ma)	Bethany Beach equivalent	New Jersey coastal plain equivalent	Oxygen isotope event
MIC 11	0	0.00	0.2	0.5					
	60	18.32	0.55	0.8					
						1.95			2.5
V11	60	18.32	2.5	3.6	2.1				
	105.5	32.16	2.8	3.8	2.3				
						0			
V10	105.5	32.16	2.8	5.2	2.3				
	130.95	39.91	3	5.3	2.4				
						1.6			4.0, 3.0
V9	131.0	39.93	4.6	5.5	3.7				
	189.8	57.77	4.9	5.8	4.0				
						1.2			5.7, 4.9
V8	189.8	57.77	6.1	7.2	4.9				
	266.4	81.20	6.4	7.5	5.2				
						0.8			
V7	266.4	81.20	7.2	7.7	5.9				
	516.3	157.37	7.7	8.0	7.6				
						0.3			
V6	516.3	157.37	8	8.0	7.6				
	671.05	205.97	8.3	8.3	7.7				
						4.5			Mi4
V5	671.05	205.97	12.8	12.9	12.3		C8	Kw3	
	815.4	248.53	13.8	14.8	13.8				
						0.3			Mi3a, b
V4	815.4	248.53	14.1	14.8	13.8		C7	Kw2c	
	984.4	300.05	14.8	15.3	14.3				
						1.2			Mi2a?
V3	984.4	300.05	16.0	16.0	15.9		C6	Kw2b	
	1085.5	330.86	16.4	16.4	16.2				
						0.9			Mi2
V2 (sr)	1085.5	330.86	17.3	19.2	17.2		C5	Kw2a	
	1100.5	335.43	17.4	19.4	17.4				
V2 (dinocyst)	1085.5	330.86	19.2	19.2	17.2			Kw1c	
	1100.5	335.43	19.3	19.4	17.4				
									unnamed
V1 (sr)	1100.5	335.43	18.2	19.8	17.4		C4	Kw1c	
	1129.8	344.36	18.4	20.0	17.5				
									Mi1b
V1 (dinocyst)	1100.5	335.43	19.5	19.8	17.4			Kw1b	
	1129.8	344.36	19.7	20.0	17.5				
	1129.8	344.36	19.8	20.0	19.4			Kw1b	
	1131.05	344.74	19.9	20.0	19.4				
						6.6			
O2	1131.05	344.74	26.5						
	1141.8	348.02	26.65						
						0.95			
O1	1141.8	348.02	27.6						
	1148.6	350.09	27.7						

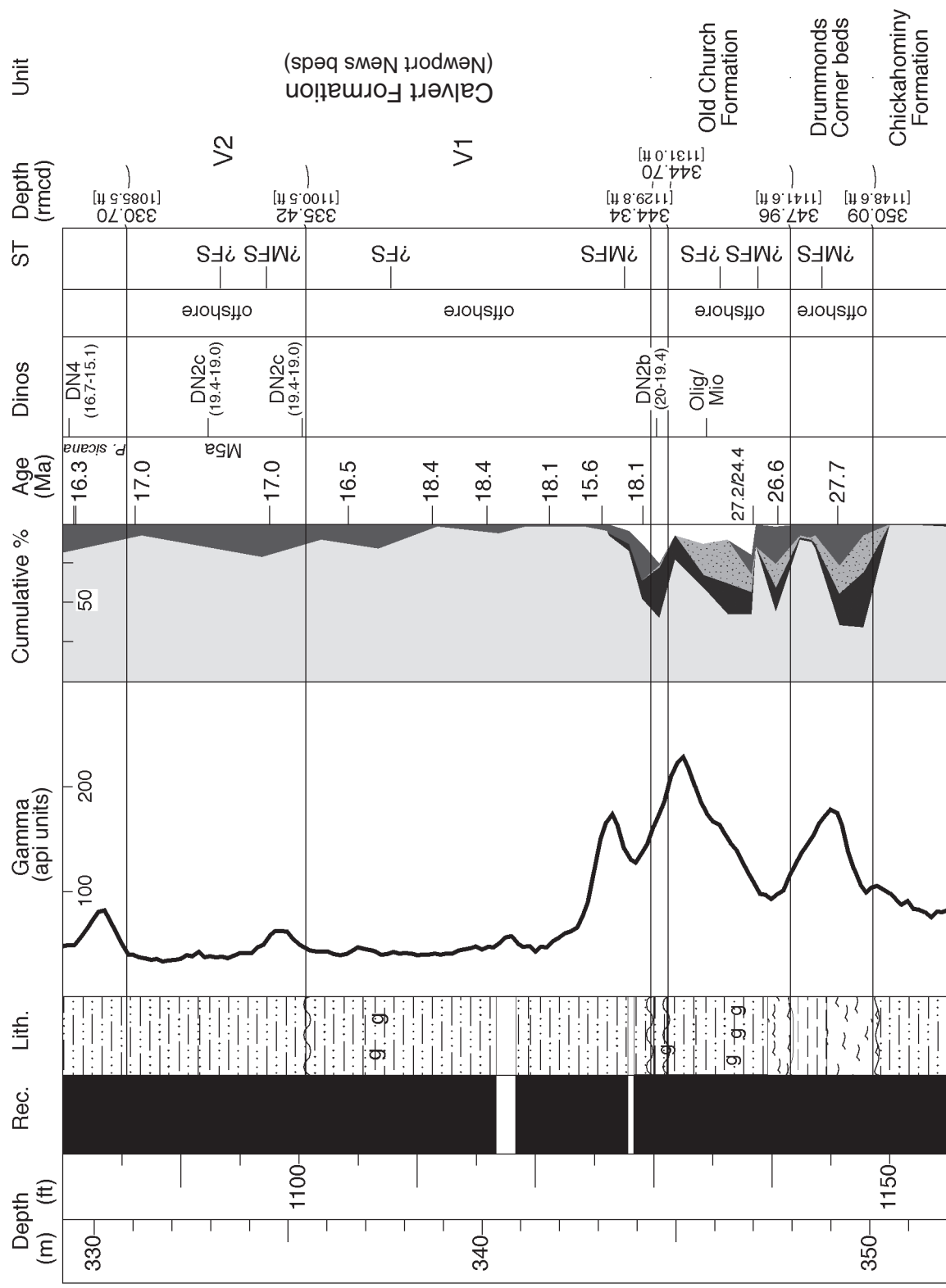


Figure 3. Recovery, lithology, gamma log, sediment components, age estimates, and systems tracts (ST) for Oligocene sequences and lower Miocene V1 and V2 sequences, Eyreville core hole. Dinos—dinoflagellates; MFS—maximum flooding surface; FS—flooded surface; *P.*—*Praeorbulina*; thin horizontal lines are sequence boundaries. Key is the same as for Figure 2.

Condensed Lower Miocene Sequences

From 344.70 to 330.70 m, three sequences are identified in Eyreville A. These sequences are placed by Edwards et al. (this volume) in the lower part of the informal Newport News beds of the Calvert Formation (see also Powars and Bruce, 1999). The lowermost sequence is very thin, and its regional significance is unknown. Age control places the upper two sequences in the early Miocene, and they are herein designated sequences V1 and V2.

From 344.70 to 344.34 rmcd, there is a thin interval, dated by dinocysts as DN2b (20–19.4 Ma) bracketed by surfaces that appear to be unconformities, and thus this interval is interpreted as a sequence (Fig. 3; Table 3). The hiatus across the lower surface is ~7 Ma in duration (ca. 27 Ma below and 20 Ma above). The contact at 344.70 rmcd is an inclined and irregular (~3 cm of relief) surface separating darker material above from lighter material below, and it is interpreted as a sequence boundary. The sequence can be divided into two parts: (1) the bottom (344.70–344.50 rmcd) consists of a very muddy glauconite sand with rare quartz, mica, phosphate, shell fragments, shark's teeth, bone fragments, and common foraminifers; this grades into (2) a mixture of material from above the upper unconformity with hard, dark, very glauconitic silt with less abundant foraminifers (344.50–344.34 rmcd). The section is heavily bioturbated, though some laminations are preserved, with burrows ranging from 1 mm to several cm in diameter.

A burrowed contact (344.34 rmcd) separating glauconitic silt below from glauconitic sand above is interpreted as a sequence boundary (Fig. 3). Above the contact, foraminifer-rich, slightly quartzose muddy glauconite sand, with shark's teeth and phosphate, is found to 344.11 rmcd, where there is a change to glauconitic, silty clay to 343.75 rmcd, above which glauconite is rare. This fining from glauconitic-rich silt to glauconite-poor clayey silt at 343.75 rmcd, associated with a secondary gamma log increase (344.4 rmcd), is interpreted as the MFS. Above the MFS, the section is diatomaceous, clayey silt to a burrowed surface at 337.63 rmcd that separates finer and darker silt below from lighter-colored foraminifera-rich, slightly glauconitic, silty clay above (337.66–335.42 rmcd). The contact is subtle, lacks an associated gamma log change, and is interpreted as a flooding surface. We name the sequence from 344.34 to 335.42 rmcd V1 and correlate it with C4 of Browning et al. (2006) (see Chronology section).

There is a burrowed contact at 335.42 rmcd with 2.2 cm of relief that separates lighter and coarser, slightly phosphatic foraminiferal silty clay with quartz grains above from finer and darker, silty clay with fewer foraminifers below; it is interpreted as a sequence boundary (Fig. 3; Table 3). The entire sequence (335.42–330.70 rmcd) consists of homogeneous, low-density, diatom-rich, slightly lignitic, silty clay with rare shell fragments. Diatoms and foraminifers are common in the cores, and the low density of the cores may be explained by high abundances of silica. A foraminiferal concentration and a burrowed contact over a darker layer at 334.33 rmcd associated with a gamma increase,

reflecting higher clay/lower biogenic content, at ~334.56 rmcd is tentatively interpreted as the MFS. A foraminiferal concentration at 333.16 rmcd close to a minor gamma-ray peak is interpreted as a flooding surface. We name this sequence V2 and correlate it C5 of Browning et al. (2006) (see Chronology section).

Middle Miocene Sequences

There are three sequences assigned to the middle Miocene and designated here V3 (330.70–300.05 rmcd), V4 (300.05–248.53 rmcd), and V5 (248.53–205.97 rmcd). The clay and silt-rich section (330.70–225.43 rmcd) is assigned by Edwards et al. (this volume) to the Calvert Formation. Edwards et al. (this volume) assign the sandy beds from 225.43 to 205.97 rmcd to the Choptank Formation.

There is a heavily bioturbated mixing zone from 330.70 to 330.41 rmcd that is interpreted as a sequence boundary (Fig. 4; Table 3). Intense burrowing continues 0.64 m into the underlying sequence associated with a gamma log increase (Fig. 4). It is difficult to distinguish between a sequence boundary and a MFS in these successions; however, carbonate content in the underlying sequence decreases up to the sequence boundary, increases and peaks immediately above the surface, and decreases again upsection, suggesting progradation/shallowing up to the surface, deepening across the surface, and progradation/shallowing above surface, which is consistent with its interpretation as a sequence boundary. There are also quartz grains above the surface, possibly indicating a sea-level lowering during the ~1 Ma hiatus (Fig. 9) and a transgressive lag during early sea-level rise, consistent with an interpretation as a sequence boundary. The position of the MFS is uncertain because of the uniform fine-grained nature of the cores. Above 330.70 rmcd, the sequence consists of uniform, bioturbated, clayey silts, with faint laminations preserved in some intervals. From 330.41 to 320.04 rmcd, clayey silt has relatively high gamma log values, with decreasing foraminiferal abundance upsection. Very low-density cores from 320.04 rmcd to the top of the sequence at 300.05 rmcd are inferred to contain abundant biosilica, mostly in the form of diatoms. Color changes across sharp surfaces at 311.63, 308.06, and 300.99 rmcd separating darker, more fossiliferous and burrowed siltier sediment above from uniform clayey silt below are interpreted as a flooding surface. There are also minor gamma peaks associated with the surfaces at 311.28 and 308.06 rmcd. Another minor gamma peak and a subtle but sharp contact at 313.90 rmcd may also represent a flooding surface. The sequence from 330.70 to 300.05 rmcd is named V3 and is correlated to sequence C6 of Browning et al. (2006) (see Chronology section).

We place a sequence boundary at 300.05 rmcd at an irregular surface (~10 cm of relief) associated with a gamma log peak (Fig. 4; Table 3). This surface separates homogeneous, faintly laminated, light-colored, clayey silt with scattered dark grains and microfossils below from dark, heavily burrowed silt with sparse, faint laminations of angular black grains, consisting of 1% glauconite and phosphatized bone fragments and shark's

teeth (300.05–299.92 rmcd), above. It is associated with an ~1.2 Ma hiatus. Above the contact, there are rip-up clasts or burrows of lighter-colored mud from underneath the contact. Above the contact (299.92–299.62 rmcd), homogeneous, light-colored mud with abundant burrows grades up to dark-colored, faintly laminated, very slightly glauconitic, calcareous clayey silt with

foraminifers (299.62–286.23 rmcd) deposited in middle neritic environments. We interpret a sharp, burrowed contact at 286.23 rmcd, associated with a gamma-ray peak, separating lighter-green, less fossiliferous silt above from darker-colored more fossiliferous silt below as the MFS. A concentration of foraminifers, dark minerals (?phosphate), and burrows at 276.1 rmcd may also

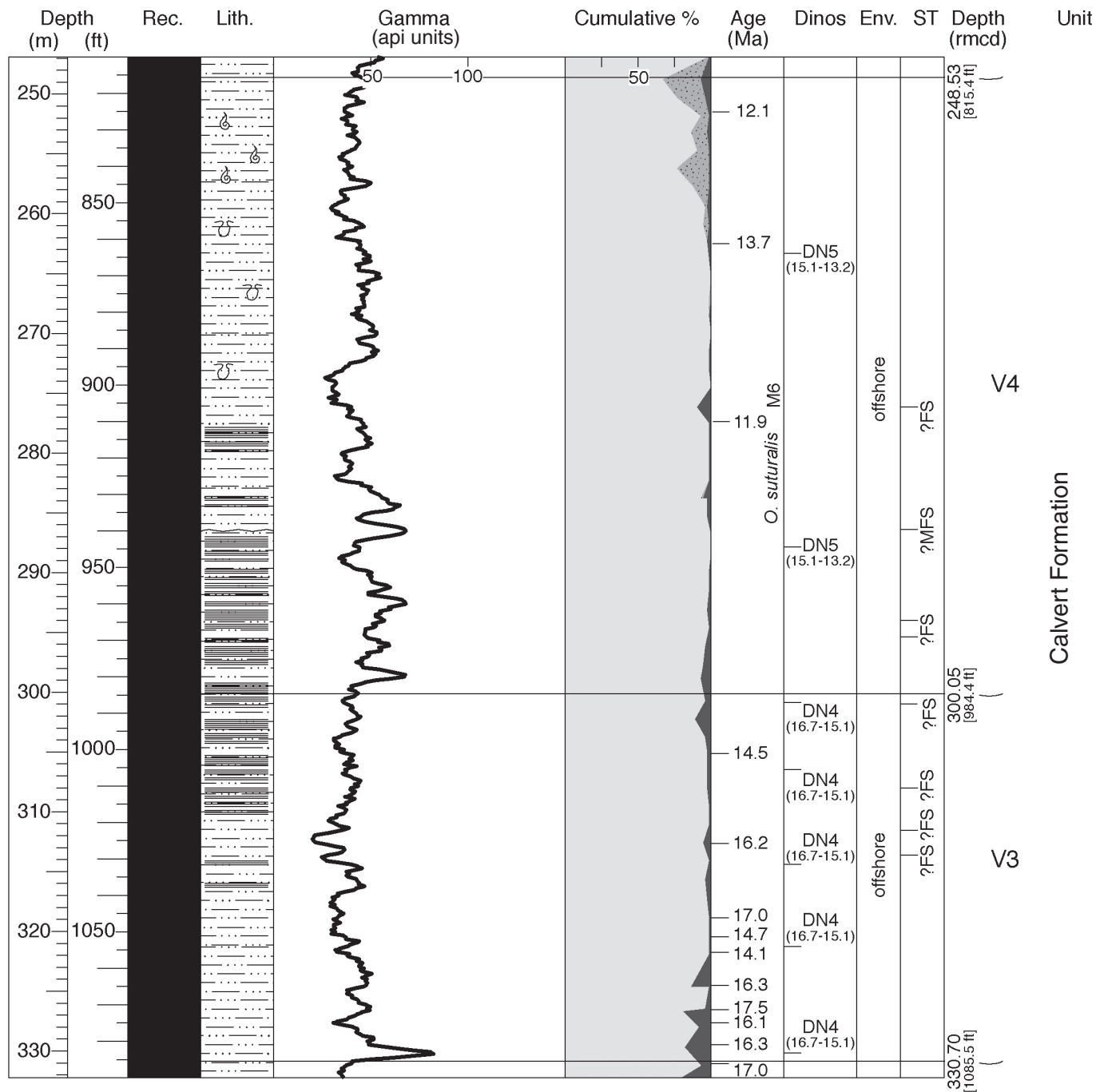


Figure 4. Recovery, lithology, gamma log, sediment components, age estimates, environment of deposition (Env.), and systems tracts (ST) for the middle Miocene V3 and V4 sequences, Eyreville core hole. Dinos—dinoflagellates; MFS—maximum flooding surface; FS—flooding surface; *O.*—*Orbulina*; thin horizontal lines are sequence boundaries. Key is the same as for Figure 2.

mark a flooding surface. Heavily burrowed surfaces at 295.28 and 294.01 rmcd associated with gamma-ray peaks are interpreted as flooding surfaces. The section from 286.23 to 262.60 rmcd consists of faintly laminated, low-density, uniform clayey silt with iron-stained burrows. Above 258.36 rmcd to the sequence boundary at 248.53 rmcd, sand increases dramatically, indicating shallowing upward in offshore environments, and the section consists of monotonous sandy clayey silt. The sequence from 300.05 to 248.53 rmcd is named sequence V4 and is correlated to sequence C7 of Browning et al. (2006) (see Chronology section).

A faint surface associated with a gamma log peak at 248.53 rmcd separates heavily burrowed monotonous clayey silt above from sandy silt below (Fig. 5; Table 3). Although this surface lacks some features of sequence boundaries, such as burrowing or rip-up clasts, we place a sequence boundary at 248.53 rmcd based on the change from sandier HST beds below to clay-rich sediments above. There is also limited evidence for a hiatus associated with this sequence boundary (Fig. 9). Another faint, irregular, iron-stained surface at 248.23 rmcd separates monotonous clayey silt with very fine sand below from bioturbated clayey silt above. The interval from 248.53 to 248.23 rmcd is interpreted as a lag deposit associated with the sequence boundary. Bioturbated clayey silt with rare laminations and less than 1% sand is found from 248.11 to 225.75 rmcd. The MFS is tentatively identified at 242.30 rmcd in a zone of little sand and relatively high microfossil content, associated with a minor gamma log increase.

The upper part of the HST (225.75–205.97 rmcd) is predominantly silty clay (Fig. 5). The section is very fine sandy, clayey silt from 224.33 to 218.75 rmcd, and sand decreases upsection to 218.75 rmcd from 21% to 5%. A contact at 218.75 rmcd is interpreted as a flooding surface, where sandier clay below passes up into clayey silt interpreted to represent a slightly deeper water environment. Sand is virtually absent in the silty clay from 219.76 to 213.66 rmcd. From 213.66 to 205.97 rmcd, the facies return to homogeneous, bioturbated, clayey, slightly sandy silt with disseminated thin shell fragments and organic debris, micaceous beds, and small pyrite concretions with weathered concentric rusty zones. We name the sequence from 248.53 to 205.97 rmcd V5 and correlate it with C8 of Browning et al. (2006) (see Chronology section).

Upper Miocene Sequences

There are three late Miocene sequences at Eyreville which we name V6 (205.97–157.32 rmcd), V7 (157.32–81.20 rmcd), and V8 (81.20–57.77 rmcd). Edwards et al. (this volume) assign the section from 255.97 to 138.41 rmcd (equivalent to sequence V6 and the lower part of V7) to the St. Marys Formation, and the section from 138.41 to 57.77 rmcd (equivalent to the upper part of sequence V7 and sequence V8) to the Eastover Formation.

A sharp contact (205.97 rmcd) marks the base of sequence V6 (Fig. 5; Table 3). The contact separates sandy silt above (205.97–205.86 rmcd) from a sandier lithology (206.19–205.97 rmcd) below containing common burrows (1 cm diam-

eter) and one large vertical burrow (12 cm) filled with sandy silt from above. Above the contact, sandy silt with burrowing and laminations extends to 205.68 rmcd, where there is a gradational change to slightly sandy silt. Very fine to coarse phosphate grains are found in the core up to 204.2 rmcd. Though the presence of very similar offshore silts above and below the contact might argue against a sequence boundary at 205.97 rmcd, this interval is marked by apparent nondeposition, possible erosion, significant burrowing, and a sandy (?winnowed then subsequently mixed by burrowing) unit in an otherwise very monotonous section. The contact at 205.97 rmcd is interpreted as a sequence boundary associated with a moderately long (~4–5 Ma) hiatus. Biostratigraphy suggests a break with zone DN6 below and DN9 above, consistent with Sr isotopic results, which suggest a hiatus of ~5 Ma across the contact. We note that this sequence from 205.97 to 157.32 rmcd does not correlate with St. Marys sequences C9 and C10 at Bethany Beach, Delaware (Browning et al., 2006), and it represents a distinctly different and younger sequence that we term V6.

A lithologic change occurs between 205.68 and 204.83 rmcd, where the clayey silt becomes slightly sandy (~5%) and shows evidence of wormy burrows. There are no other obvious changes in the section, and 204.83 rmcd may be the MFS (Fig. 5). Uniform, very dark greenish gray, very clayey silt to very silty clay with virtually no sand to a trace of sand (especially 181.51–176.78 rmcd) and scattered plant fragments occurs from 204.83 to 167.64 rmcd. Common small (up to 2 cm) pyrite nodules that oxidize to rusty concentric ring structures occur from 206.19 to 204.43 rmcd and from 189.3 to 184.29 rmcd. Scattered shells first appear at 191.39 rmcd, becoming common upsection to 163.00 rmcd, with a zone of more common shells at 179.74–179.44 rmcd. The top of the sequence (167.64–160.87 rmcd) is slightly coarser, consisting of very slightly sandy, clayey silt with traces of mica and no obvious shells. From 160.87 rmcd to the sequence boundary at 157.32 rmcd, there is a zone of shelly muddy sand with scattered large, thick bivalve shells that become more common upsection above 159.62 rmcd. The gamma log signature of these sandy silts is noticeably lower than the signature of the sediments below or above. This slight increase in sand and shells at the top is interpreted to represent shallowing at the top of the HST in an offshore environment.

A very thick and environmentally complex sequence is found from 157.32 to 81.20 rmcd and is termed V7 (Fig. 6; Table 3). A contact at 157.32 rmcd, associated with a shift in the gamma log to higher values, separates sandy, slightly clayey silt above from very sandy, very slightly glauconitic silty clay below. The decrease in sand reflects a shift to a deeper-water environment, and the surface at 157.32 rmcd is interpreted as a sequence boundary.

The section from 157.32 to 138.41 rmcd is a heavily bioturbated, fining-upward succession of fine-grained sediments (Fig. 6). From 157.32–156.77 rmcd, the section is heavily bioturbated, slightly sandy, slightly clayey silt with scattered shell debris (to 4 mm). From 157.23 to 149.35 rmcd, silty clay to

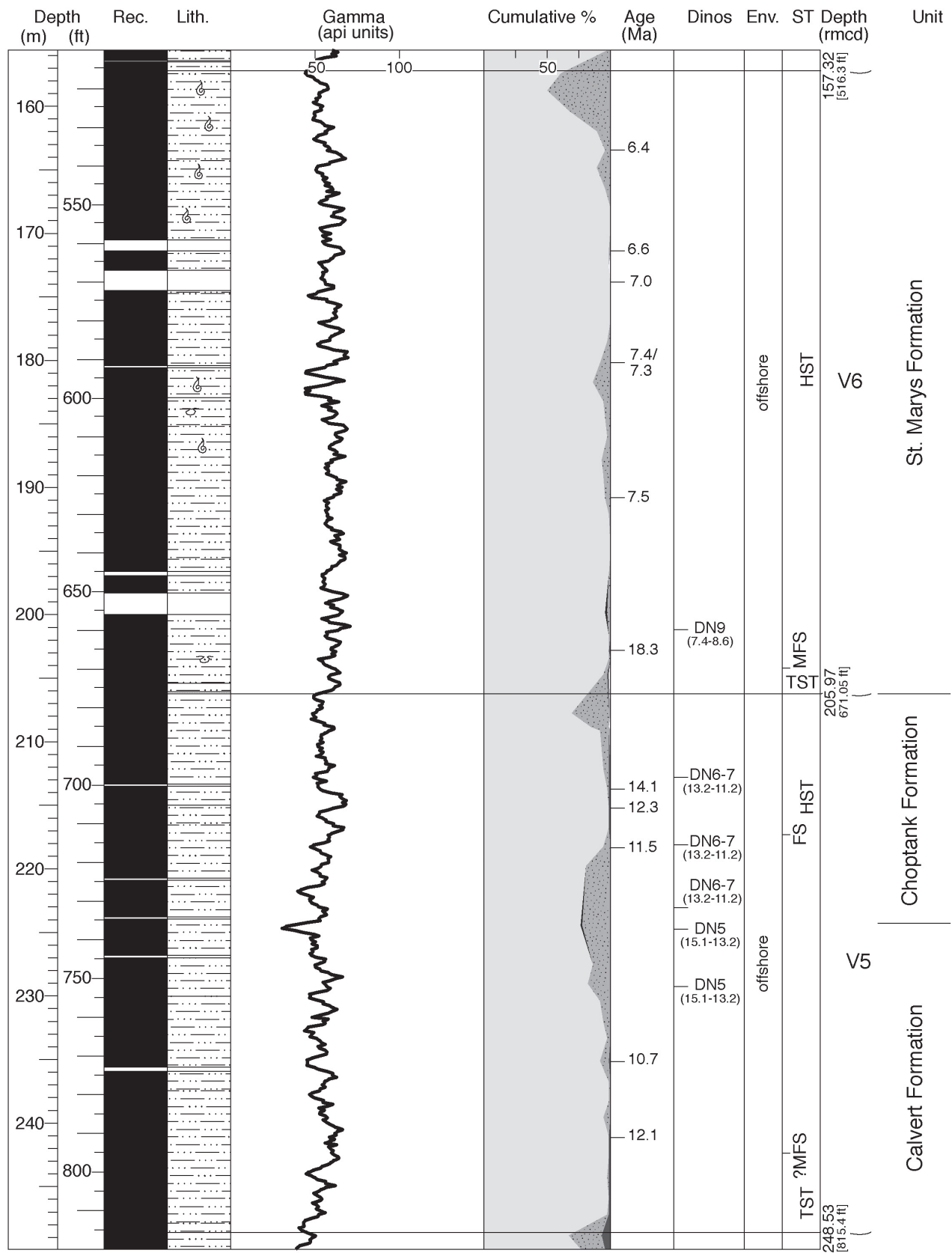


Figure 5. Recovery, lithology, gamma log, sediment components, age estimates, environment of deposition (Env.), and systems tracts (ST) for the lower Miocene V5 sequence and upper Miocene V6 sequence, Eyreville core hole. Dinos—dinoflagellates; MFS—maximum flooding surface; TST—transgressive systems tract; HST—highstand systems tract; FS—flooding surface; thin horizontal lines are sequence boundaries. Key is the same as for Figure 2.

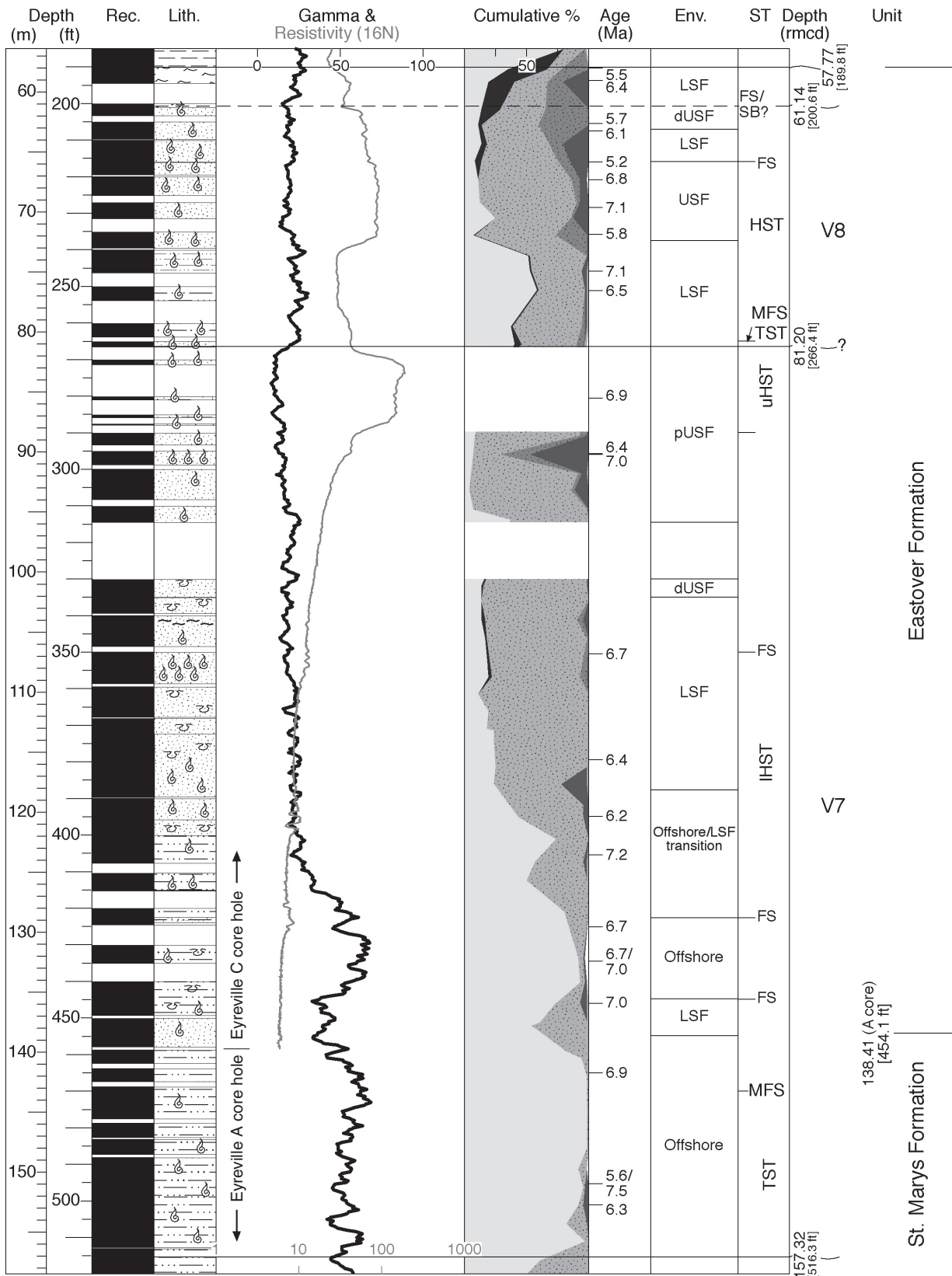


Figure 6. Recovery, lithology, gamma (api units) and resistivity (ohm-m) logs, sediment components, age estimates, environment of deposition (Env.), and systems tracts (ST) for the upper Miocene V7 and V8 sequences, Eyreville core hole. MFS—maximum flooding surface; TST—transgressive systems tract; HST—highstand systems tract; IHST—lower highstand systems tract; uHST—upper highstand systems tract; FS—flooding surface; LSF—lower shoreface; USF—upper shoreface; dUSF—distal upper shoreface; pUSF—proximal upper shoreface; thin horizontal lines are sequence boundaries. Key is the same as for Figure 2.

clayey silt contains very little sand (5%–8%). Shells, particularly bivalves, are more abundant from 151.57 to 151.07 rmcd. From 149.35 to 138.41 rmcd, the lithology is a relatively homogeneous, slightly micaceous, slightly shelly (thick bivalves or *Turritella*) clayey silt with virtually no sand. The section from ~143.56 to 142.95 rmcd has common visible foraminifers, sulfur blooms, and postdrilling gypsum crystals associated with a gamma-ray maximum and is interpreted as the MFS. The section was deposited in an offshore environment. Thus, most of the sequence (viz. from 142.95 to 81.20 rmcd) is interpreted as the HST.

A sandy lower shoreface unit from 138.41 to 136.79 rmcd (Fig. 6) consists of slightly micaceous silty, very fine sand, with up to 2% very fine silt-sized opaque heavy minerals (most likely lignite). The section is burrowed to cross-laminated, and physical structures dominate. The upsection change from silt to burrowed sand indicates a distal lower shoreface environment. The top of the sand is a flooding surface that appears abrupt on the hole A gamma log.

Sediments from land surface to 139.57 m are described from the C core (Fig. 6). Heavily bioturbated, clayey silt to silty clay with rare laminations and sparse scattered shells and shell fragments occurs from 135.58 to 128.78 rmcd and were deposited in offshore environments. The section changes from grayish brown clay at the bottom to gray clay with more silt at the top (135.58–134.11 rmcd). Discrete burrows (millimeter and smaller, sand-filled burrows, pyritized burrows, and incipient nodules) are rare in an otherwise homogeneous section. Common pyrite nodules occur from 132.19 to 132.13 rmcd, and nodules or cemented beds with bivalve molds occur from 129.24 to 128.78 rmcd. We place a flooding surface at 128.78 rmcd at the top of the indurated zone.

Slightly coarser beds return above 128.78 rmcd. From 128.78 to 121.01 rmcd, the section consists of very fine sandy silt containing scattered pockets of shell fragments and large whole shells (Fig. 6). The section is bioturbated with hints of laminations. Thin sandy zones at 128.12–128.11 and 126.58–126.49 rmcd contain crumbly sand and concretions with large shells, including a *Cliona* bored shell in the upper cemented zone. The section from 121.10 to 120.61 rmcd (across a coring gap) is a carbonate (dolomitic) cemented, silty, very fine sandstone with shell molds. The sediment generally coarsens above 120.61 rmcd to shelly, clayey silt to silty sand at 119.63 rmcd and to very fine silty sand at 118.51 rmcd. From 120.61 to 118.51 rmcd, the core alternates between silty, very shelly sand beds and very silty sand. This change (128.78–118.51 rmcd) from finer to coarser sediments represents environments transitional between offshore and lower shoreface, where the sand represents shallower environments and the silt represents deeper environments.

The sediments above 118.45 rmcd are predominantly sand (Fig. 6). The lithology from 118.45 to 109.18 rmcd is heavily bioturbated, very slightly micaceous, slightly shelly, slightly glauconitic (1%–2%), silty, fine quartz sand with more common shells from 118.45 to 116.53 rmcd and scattered shell fragments from 112.62 to 109.18 rmcd. From 118.41 to 111.25 rmcd sand-filled burrows are conspicuous, and mud-lined burrows (1–2 cm)

are common from 111.25 to 110.19 rmcd. The section from 109.18 to 106.68 rmcd consists of shell-rich, muddy, very fine to fine sand with 1%–2% glauconite. Shells include large phosphatized (2–5 cm) bivalve, gastropod, and barnacle fragments that vary in color from white to black. The section from 106.68 to 102.11 rmcd is very fine to fine silty sand with scattered shell fragments and clay-lined burrows. Above 102.11–100.58 rmcd, the section becomes silty, well-sorted fine quartz sand with fewer shells and glauconite (5%–10%), and it is less bioturbated than below. The section from 118.45 to 102.11 rmcd was deposited in lower shoreface environments that become progressively shallower and sandier upsection. The section from 102.11 to 100.58 rmcd was deposited in distal upper shoreface environments. A slight increase in glauconite across a coring gap (106.68–106.18 rmcd) associated with a sharp gamma log increase suggests a water depth increase. Because there is no large change in lithology and no major deepening of paleoenvironments across the gap, we interpret the change in the 106.68–106.18 rmcd coring gap as a flooding surface.

A unit of fine to very fine quartz sand with abundant shell fragments is encountered (Fig. 6) between 95.83 and 88.39 rmcd. The interval contains a variety of small shell beds, including an interval of very shelly, quartz sand with large (2–4 cm) shell fragments and whole bivalve shells from 90.22 to 89.92 rmcd. There is a gradational change from well-sorted silty fine sand below 94.49 rmcd to shelly, fine sand above. Poor recovery characterizes the indurated sands (88.39–81.20 rmcd) of the upper part of the HST. Dolomitized sandstone alternates with a soft matrix between 88.39 and 81.20 rmcd. The sandstone consists of a fine- to medium-grained matrix of shells and quartz sand with abundant large shell fragments. The section from 95.83 and 81.20 rmcd was deposited primarily in proximal upper shoreface environments. We place a sequence boundary at 81.20 rmcd, where there is a shift in lithology from shelly fine sand above to indurated fine- to medium-grained sand below associated with a dramatic gamma log decrease and resistivity log increase (82.30–81.20 rmcd).

We term the overlying sequence from 81.20 to 57.77 rmcd V2 (Fig. 6; Table 3). Virtually all of the sequence is HST, with a very thin TST from 81.20 to 80.77 rmcd, a thick lower HST silt (80.77–72.54 rmcd), and a thick sandy upper HST. Glauconite decreases upsection from 3%–5% at 81.20 rmcd to a trace at 80.77 rmcd. We interpret the decrease in glauconite as the MFS of the sequence. The HST occurs from 80.77 to 72.54 rmcd and consists of bioturbated slightly sandy silt containing whole shells including *Isognomon*. The presence of sand indicates deposition above storm wave base. The fact that the sand is found with abundant silt and is bioturbated shows that waves only intermittently disturbed and winnowed sediments on the bottom. We conclude the sandy silts were deposited above storm wave base but below fair-weather wave base in lower shoreface environments. Changes in shell content mark the section between 72.54 and 61.14 rmcd, ranging from scattered shells increasing in abundance upsection (70.53–68.28 rmcd) to shell

hash with fragments of large thick shells (68.28–65.81 rmcd), to more common, whole shells (including common *Mulinia*; 65.81–63.09 rmcd), to scattered shells (63.09–61.26 rmcd), to shelly, slightly glauconitic (to 3%), silty, very fine quartz sand (61.26–61.14 rmcd). Bivalves include *Isognomon*, *Pecten*, and oysters. The changes in shell material in a sandy lithofacies are interpreted to reflect changes in environment. In general, the amount of shell material increases upsection from 68.28 to 65.81 rmcd, and the transition at 65.81 rmcd may mark a flooding surface. Glauconite reworked from older strata ranges from 3% to 4% above 67.36 rmcd. The sands from 72.39 to 65.81 rmcd are less silty and shellier than the sands from 80.77 to 72.54 rmcd, indicating deposition in a higher-energy environment, likely above fair-weather wave base. We interpret these sediments as upper shoreface deposits. The appearance of more common, small, whole shells from 65.81 to 63.09 rmcd is inferred to indicate a quieter environment, with deeper-water levels upsection across the 65.81 rmcd surface, and the section between 65.81 and 63.09 rmcd was deposited in proximal lower shoreface environments. The section from 63.09 to 61.14 rmcd was deposited in distal to proximal upper shoreface environments.

Above a burrowed contact at 61.14 rmcd, the section consists of shelly, clayey glauconite-quartz sand with increasing quartz downsection (Fig. 6; Table 3). The upper part is somewhat muddier, reflecting bioturbation from above. The section from 61.14 to 57.77 rmcd was deposited in lower shoreface environments. Thus, there is deepening across the contact at 61.14 rmcd that is either a sequence boundary or a flooding surface. In the absence of criteria clearly indicating a sequence boundary, we interpret it as a flooding surface.

Pliocene Sequences

Pliocene sediments in the Eyreville core hole are placed in three sequences. Sequence V9 (57.77–39.93 rmcd) is placed by Edwards et al. (this volume) into the Sunken Meadow and Rushmere Members of the Yorktown Formation. Sequence V10 (39.93–32.16 rmcd) is placed by Edwards et al. (this volume) into the Morgarts Beach Member of the Yorktown Formation. Sequence V11 (32.16–18.32 rmcd) is placed by Edwards et al. (this volume) into the Chowan River Formation.

There is a sharp contact in the core at 57.77 rmcd interpreted as a sequence boundary because of the sharp facies shift from lower shoreface below to lagoonal or estuarine above (Fig. 7; Table 3). The interval from 57.77 to 55.81 rmcd consists of clayey, slightly sandy silt with laminations, rare mica, common pollen, very few dinoflagellates, and very common plant debris (Fig. 7). Common pollen and plant debris is unusual in a middle neritic clay, and the environment of deposition is interpreted as estuarine or lagoonal. The regional significance of this section is not certain, and we consider it to be the lowermost facies of the overlying sequence.

There is a facies shift across a contact at 55.81 rmcd with heavy bioturbation (with burrows up to 2 cm in diameter), and a

basal glauconitic interval above the contact, though there are no obvious rip-up clasts (Fig. 7). The section below the contact is significantly shallower (lagoon/estuary) than above (distal lower shoreface), and we interpret this contact as a sequence boundary. We name the sequence between 57.77 and 39.93 rmcd V9. The section from 55.81 to 55.69 rmcd is a transgressive lag in which glauconitic medium sand contains large burrows filled with the underlying clay. The glauconitic sand becomes very phosphatic between 55.69 and 55.47 rmcd. The section changes to slightly glauconitic sandy silt (54.19–53.98 rmcd). We place the MFS at 53.98 rmcd at the top of the glauconitic silt at a gamma-ray peak. Above the glauconite silt, the section changes upward to heavily bioturbated, shelly to very shelly, fine to medium quartz sand (53.98–48.10 rmcd). The environment of deposition of the section from ~52.73 to 48.10 rmcd is primarily lower shoreface, though it is progressively shallower water upsection and probably represents distal lower shoreface environments below a gamma log kick at 51.21 rmcd.

There is a contact at 48.10 rmcd at the base of a shelly zone; this contact is either a flooding surface (favored by a decrease in coarse sand) or a storm event because there does not appear to be a significant change in environment/facies across the contact (Fig. 7; Table 3). From 48.10 to 47.35 rmcd, a sandy shell bed contains bivalve fossils including *Cardium* and *Pecten*. Shells are more abundant in the fine sand from 47.35 to 44.47 rmcd, with bivalves and large barnacles. The section from 44.47 to 43.07 rmcd has scattered shells and shell fragments, and it coarsens to slightly silty, fine sand. The section from 43.07 to 39.93 rmcd consists of moderately sorted fine (10% medium) sand with traces of glauconite and opaque heavy minerals. The section is bioturbated throughout, and laminations are preserved in a few intervals (e.g., 43.07–42.67 rmcd). Foraminifers and ostracods are largely absent from 45.72 to 39.62 rmcd. The environment of deposition for the section from 48.10 to 39.93 rmcd is lower shoreface.

There is a contact at 39.93 rmcd at the base of a shelly zone (39.93–38.40 rmcd) containing numerous dark fragments and an associated gamma peak. We interpret this contact as a sequence boundary (Fig. 7). We name the sequence from 39.93 to 32.16 V10. Shells are chalkier from 39.90 to 39.53 rmcd than they are above, which may indicate exposure on the ocean floor. Glauconite is common from 38.40 to 37.64 rmcd. The glauconitic section is tentatively interpreted to mark the MFS, which is placed at 37.80 rmcd, associated with a gamma log kick. The section from 38.56 to 33.53 rmcd consists of very shelly, slightly glauconitic, silty, poorly sorted, very fine to medium quartz sand with scattered sandy shell beds. Most of the shells are fragments, though whole specimens of *Mulinia*, razor clams, and other species occur. The depositional environment of the section from 39.93 to 33.53 rmcd is interpreted as lower shoreface that shallows upward above the MFS.

There is a lithologic change across a coring gap at 33.53–31.50 rmcd, with medium-coarse quartz sand with larger and more abundant shells below and finer-grained muddy sand

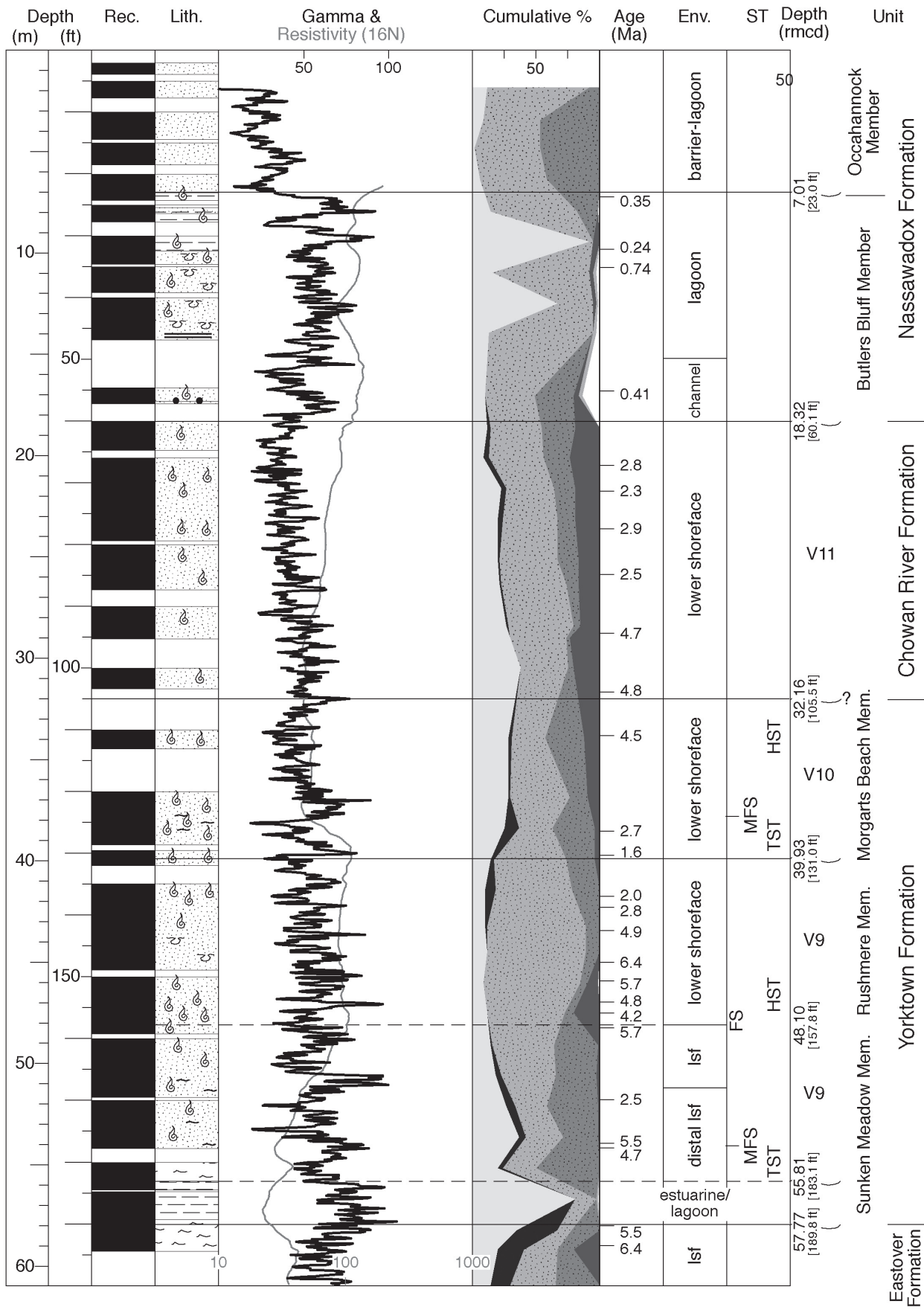


Figure 7. Recovery, lithology, gamma (api units) and resistivity (ohm-m) logs, sediment components, age estimates, environment of deposition (Env.), and systems tracts (ST) for the Pleistocene V9, V10, and V11 sequences and the Pleistocene MIC11 sequence, Eyreville core hole. MFS—maximum flooding surface; TST—transgressive systems tract; HST—highstand systems tract; lsf—lower shoreface; FS—flooding surface; thin horizontal lines are sequence boundaries. Key is the same as for Figure 2.

immediately above (Fig. 7). The section below coarsens upward to the contact, and the section above the sequence boundary is finer-grained and coarsens upward consistent with a basinward shift in facies. We place a sequence boundary in the coring gap at 32.16 rmcd at a prominent gamma log kick.

From 31.50 to 18.32 rmcd (Fig. 7), the section is uniform, slightly micaceous, fine sand with a few percent opaque heavy minerals, traces of glauconite, scattered shells, and partly preserved small-scale (0.5–3 cm) cross-stratification. This sequence is here termed V11 (32.16–18.32 rmcd). Shells in the section are primarily small bivalves, with razor clams and a scaphopod noted at 28.68 rmcd. From the base of the sequence to 21.34 rmcd, more laminated intervals alternate with more bioturbated intervals. Laminations and cross-laminations are more prominent from 29.05 to 27.43 rmcd, and shell concentrations occur at 23.65–23.62 and 21.15–21.12 rmcd. The sand content increases slightly above 24.38 rmcd. The slight coarsening upsection from 31.50 to 18.29 rmcd is reflected in the gamma log as slightly decreasing values upsection. The shelly sands were deposited in a lower shoreface environment that shallow upsection.

Pleistocene Sequence

Pleistocene sediments are placed into two loosely dated sequences. Edwards et al. (this volume) place the lower sequence (18.32–7.01 rmcd) into the Butlers Bluff Member of the Nassawadox Formation and the upper sequence (7.01–1.19 rmcd) into the Occahannock Member of the Nassawadox Formation.

Above a coring gap (18.32–17.43 rmcd), the lithology shifts to slightly shelly, fine sand (Fig. 7). A gamma log increase suggests the contact is at or near 18.29 rmcd. A red micaceous sandstone cobble and a 4 cm quartzite pebble occur from 17.43 to 17.34 rmcd, marking a channel lag in the base of a paleochannel. Gravel at 17.34–17.31 rmcd is very poorly sorted (ranging from fine sand to 1-cm-diameter pebbles) and grades to poorly sorted, shelly, medium sand with thicker shells to 16.64 rmcd. Above a large coring gap (16.64–14.30 rmcd), the section is bioturbated, variably silty, shelly, fine to very fine sand to 10.67 rmcd, where it changes to heavily burrowed, shelly, slightly silty, fine to very fine sand that continues to an irregular surface at 9.91 rmcd. From 9.91 to 7.01 rmcd, the section consists of interbedded shelly silty sand, sandy silt, and clayey silt. Shells from 14.30 to 7.01 rmcd represent a low-diversity fauna composed largely of small (~3 mm), thin-walled bivalves (*Mulinia*), dinocysts (*Polysphaeridium*; warm, salinity tolerant), and benthic foraminifers (*Elphidium*). We interpret the section from 14.30 to 7.01 rmcd as possibly lagoonal or estuarine. The sequence from 18.32 to 7.01 rmcd is dated as ca. 400 ka and thus correlates with marine isotope chron 11 (see Chronology section).

Across a sharp contact at 7.01 rmcd, tentatively interpreted as a sequence boundary, there is a lithologic change to sand that is cleaner at the base and muddier at top (Fig. 7). From 7.01 to 6.77 rmcd, the section is a poorly sorted, medium sand that grades up (6.77–6.52 rmcd) to poorly sorted, very slightly silty,

fine sand. The section changes to muddy fine sand with a trace of mica and 1%–2% opaque heavy minerals (6.52–6.10 rmcd); fine sand with traces of mica, a few percent opaque heavy minerals, and thin mud drapes (5.64–5.30 rmcd); interbedded mud (0.5–1 cm thick) and fine sand (2–4 cm thick) (5.30–5.09 rmcd); silty fine to medium sand with mud drapes (5.09–4.85 rmcd); and, at the top, slightly silty, orange, fine to medium sands with a few percent opaque heavy minerals (4.85–4.57 rmcd). Because of the rapidly changing nature of the sediments, the section is inferred to represent nearshore environments, and the section above the 7.01 rmcd contact is interpreted as a barrier-lagoon complex; these sands may represent back-barrier environments.

The section from 4.39 to 1.19 rmcd (Fig. 7) contains two fining-upward successions. The succession from 4.39 to 3.05 rmcd has medium to fine sand with 1%–2% opaque heavy minerals that fines slightly upsection. Leisegang banding in this interval may follow cross-bedding. Medium sand with coarse sand stringers between 2.35 and 2.07 rmcd fines up to silty fine sand (2.07–1.52 rmcd). These fining-upward sections are interpreted as small channels deposited in an estuarine environment.

We lack age control on this sequence other than it is superposed above marine isotope chronozone 11 and predates the Holocene, which suggests correlation to marine isotope chron 5e.

PALEOWATER DEPTH INTERPRETATION

Paleowater depths in the Eyreville core were determined using integrated lithofacies and qualitative benthic foraminiferal biofacies analysis (Fig. 8). In shallow-water sections, sedimentary facies and facies successions show relative water depth changes that can be assigned absolute paleowater depths. In general, sediments in proximal upper shoreface environments were deposited in 2–5 m paleodepth. Distal upper shoreface deposits represent water depths down to fair-weather wave base (~5–10 m paleodepth). Lower shoreface deposits accumulated below fair-weather wave base but above storm wave base (~10–30 m). Offshore sediments were deposited in water depths greater than 20–30 m paleodepth below storm wave base.

For middle to outer neritic environments (>20 m paleodepth), changes in benthic foraminiferal assemblages are used to interpret paleowater depth histories (Browning et al., 2006, 2008). We relied on the benthic foraminiferal biofacies zonation of Miller et al. (1997): The *Elphidium* biofacies is an indicator of nearshore paleoenvironments with 10 m or less water depth. The *Hanzawaia* biofacies is an indicator of inner neritic paleodepths (from 10 to 25 m). The *Pseudonion* biofacies characterizes paleodepths of 25–50 m. The *Bulimina* biofacies characterizes offshore middle neritic (50–80 m) paleodepths. The *Uvigerina* biofacies characterizes offshore middle to outer neritic paleodepths (>75 m).

Generally, paleowater depths are greatest in the Chickahominy Formation and tend to shallow upsection (Fig. 8). The Chickahominy Formation is dominated by *Bulimina* spp. and agglutinated foraminifers that are interpreted to have lived in high-stress environments (Poag, this volume). Because this is not entirely

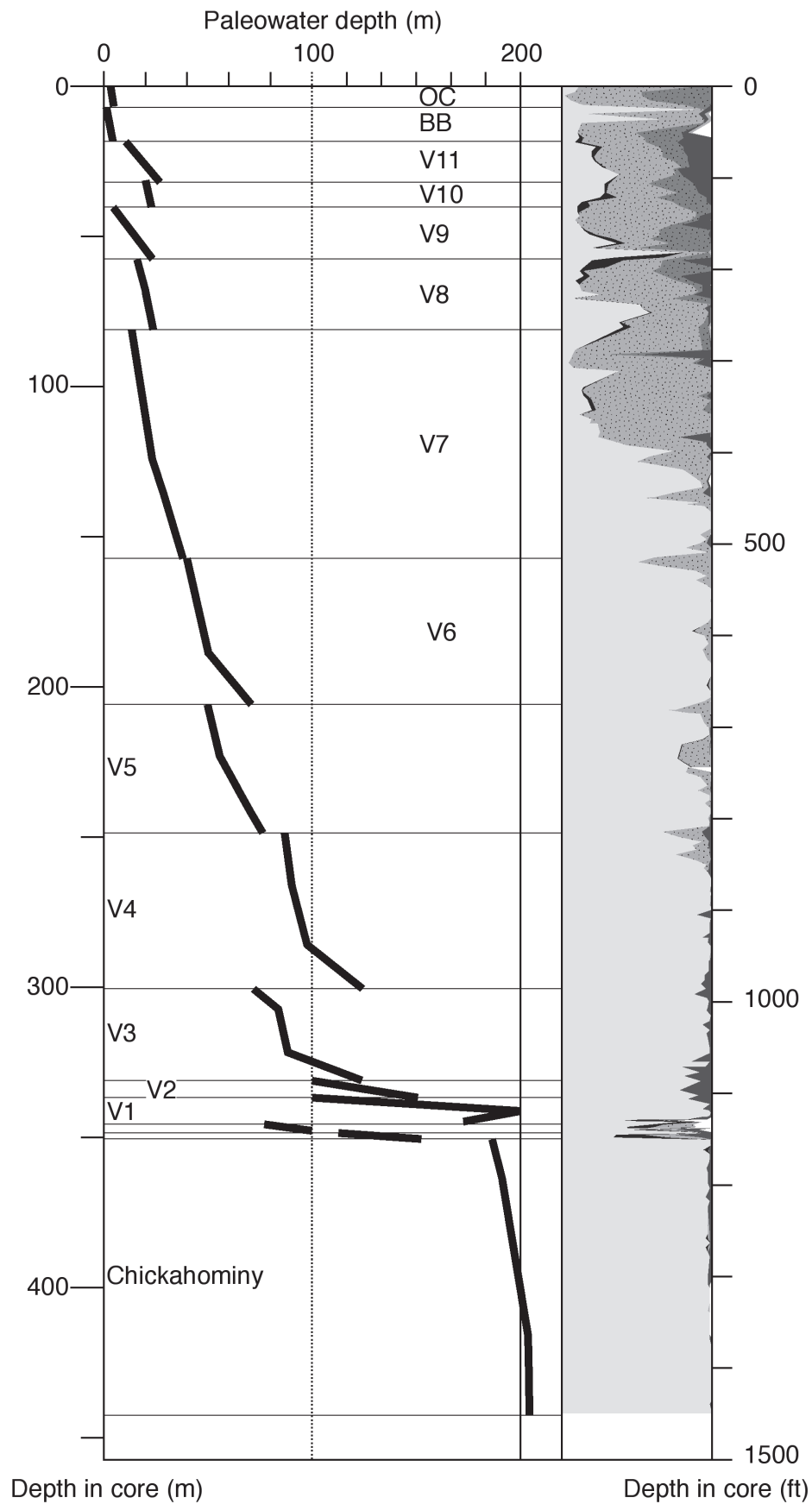


Figure 8. Paleowater depth estimates for the sequences recognized in the Eyreville core hole.

a normal marine environment, paleodepth interpretation using benthic foraminifers is difficult. The dominance of *Bulimina* suggests deep-water outer neritic (100–200 m) or upper bathyal (200–600 m) water depths. Oligocene samples are dominated by *Uvigerina*, suggesting paleodepths of 75–100 m. Miocene sequence V1 contains abundant *Uvigerina* along with *Rectuvigerina*, which is typically found in outer neritic paleodepths. This suggests that sequence V1 was deposited in paleodepths ranging from 175 to 200 m at the bottom shallowing to 100 m at top. Abundant *Uvigerina* in sequences V2, V3, and V4 suggest middle neritic paleodepths (75–100 m). Sequence V5 contains a *Uvigerina*-dominated fauna (100 m) at the base, and it shallows to a *Pseudononion*-dominated fauna (25–50 m) at the top. Sequence V6 shallows from a *Bulimina*-dominated fauna (50–80 m) at the base to *Pseudononion* on the top.

Younger sequences were largely deposited above storm wave base and contain few foraminifers (Fig. 8). Ea 1 and 2 were deposited in lower shoreface environments to upper shoreface environments (20–5 m; Fig. 8). V9 and V10 were deposited in lower shoreface environments (20–10 m). Sequence V11 contains *Hanzawaia* (~25–10 m), which is in agreement with lithofacies evidence of lower shoreface environments (20–10 m). The uppermost Pleistocene sequence contains a benthic foraminiferal fauna dominated by *Elphidium* (>10 m) consistent with the lithologic interpretation of a barrier-lagoon complex.

CHRONOLOGY AND STRONTIUM ISOTOPIC STRATIGRAPHY

Strontium isotope stratigraphy was the main tool used to date the sequences in the Eyreville core holes. The strontium isotopes were augmented using planktonic foraminifer and dinocyst biostratigraphy (Table 4).

Planktonic Foraminifers

Fifty samples between 440.79 and 350.92 rmcd from the upper Eocene Chickahominy Formation were examined for planktonic foraminiferal biostratigraphic purposes. Planktonic foraminiferal preservation ranged from poor to very good and generally increased downhole, but it is inferior to that illustrated in Poag and Commeau (1995) of the southwestern Salisbury Embayment. Sample 436.18 rmcd exhibited excellent preservation and many forms glassy under the light microscope, suggesting unaltered primary calcite. Benthic foraminifers are abundant throughout. Samples were dominated by the planktonic foraminiferal species of *Subbotina* and *Turborotalia* and showed no evidence of reworking. Ostracods, radiolarians, and dinoflagellates were also present. The Chickahominy Formation is divided into two biostratigraphic zones.

Globigerinatheka index is found consistently between 440.3 and 400.72 rmcd, indicating foraminiferal biozone E15 (older than 34.3 Ma). Foraminifers are abundant throughout this interval, and preservation is generally good to very good. *Globigeri-*

natheka semiinvoluta was not encountered, suggesting that the base of the interval studied is younger than 35.8 Ma.

The interval from 399.41 to 350.92 rmcd contained abundant planktonic foraminifers. The presence of *Hantkenina alabamensis*, *Cribohantkenina inflata*, and *Turborotalia cocoaensis* in the absence of *Globigerinatheka* indicates that this is upper Eocene biozone E16, corresponding to 33.7–34.3 Ma. The 63–125 μ m size fraction contained abundant tenuitellids.

Planktonic foraminifers were common to abundant in the Miocene V2 and V3 sequences and in the base of the V4 sequence, and marker species helped date these sequences. Planktonic foraminifers were rare in the sequences above 299 rmcd, and most specimens represent long-ranging taxa. The highest occurrence (HO) of *Catapsydrax unicava* at 334.06 rmcd indicates sequence V2 is Zone M3. The *Praeorbulina* lineage is represented in sequence V3 and the base of sequence V4. The lowest occurrences (LO) of *Praeorbulina sicana* and *Praeorbulina glomerosa curva* are at 329.61 rmcd and 312.72 rmcd, respectively. *Praeorbulina glomerosa glomerosa* LO is at 305.13 rmcd, and *Praeorbulina glomerosa circularis* LO is above the 299.92 rmcd sequence boundary at 299.01 rmcd. At 263.87 rmcd, *Globorotalia praemenardii* indicates assignment to Zones M7–M9. A specimen of *Globorotalia pleisiotumida* (Zones M13–PL1) was encountered at 203.48 rmcd.

Strontium Isotopes

Nearly the entire Miocene-Pliocene was sufficiently fossiliferous for mollusks and foraminifers for Sr isotopic analysis (Table 2). Sr isotope stratigraphy has high resolution in the early to earliest middle Miocene (ca. 24–15 Ma) because of high rates of increase in $^{87}\text{Sr}/^{86}\text{Sr}$, but it has lower resolution due to lower rates of increase in the later Miocene to Pliocene. The Eyreville core hole recovered ~50 m of strata dated 27.4–15.5 Ma (350–300 rmcd), and a thick section dated between 14.8 and 2.5 Ma (300–18.3 rmcd). Because of the lower resolution (± 1.2 Ma or worse; Oslick et al., 1994), results from this upper section did not cluster together well within a sequence and sometimes disagreed with the available biostratigraphy. In making age/depth plots, correlation lines utilized as much of both the biostratigraphic data and Sr age estimates as possible. Generally, Sr age estimates from the Eyreville cores that used foraminifers gave results that were more reproducible, while Sr age estimates using mollusk shells had more scatter. Sr isotopic changes in the Eocene are small and do not allow for age resolution beyond what is provided for by biostratigraphy.

Oligocene Sequences

The two thin Oligocene sequences in the Eyreville core contain little carbonate and are difficult to date using Sr isotopes (Fig. 9). Only one Sr age estimate (27.7 Ma at 349.18 rmcd) was obtained from the lower sequence (350.09–348.02 rmcd), and the sequence is estimated to indicate an age of 27.7–27.6 Ma, assuming a sedimentation rate of 20 m/Ma typical of New Jersey

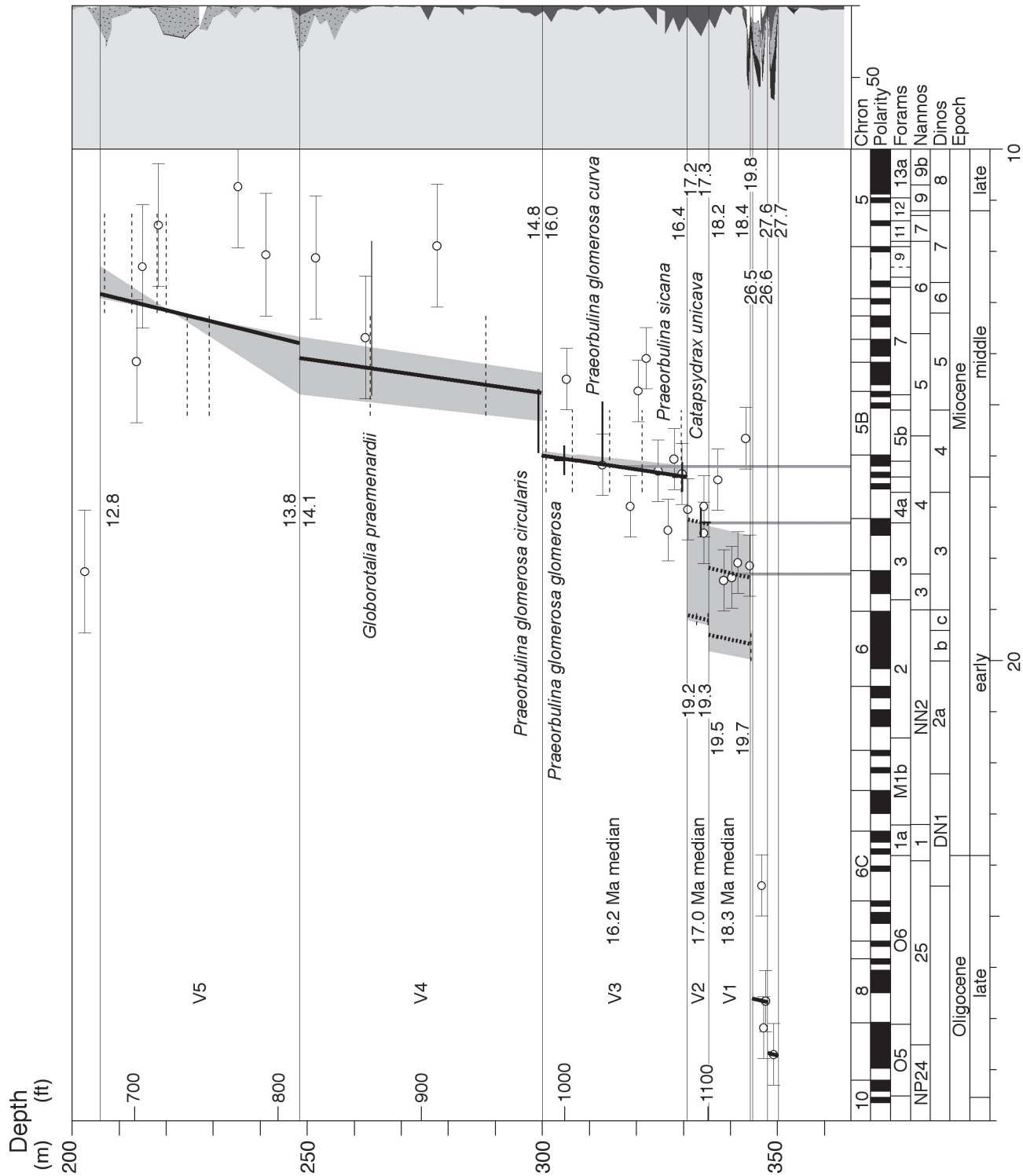


Figure 9. Age-depth plot showing the distribution through time of the Oligocene through middle Miocene sequences in the Eyreville core hole. V1–V8 refer to sequences discussed in the text. Open circles are strontium age estimates with errors. Thin dashed lines are age estimates for dinocyst samples. Thin horizontal lines are inferred unconformities. Thick black line is the preferred age estimate; thick dashed line is an alternate age estimate. Shaded areas behind age estimates represent age uncertainties. Forams—planktonic foraminiferal zones; Nannos—calcareous nannoplankton zones; Dinos—dinoflagellate zones. Time scale is after Berggren et al. (1995). Key for lithology column is the same as for Figure 2.

Oligocene sequences (Pekar et al., 2000). This suggests correlation to sequence O4 in New Jersey (Pekar and Miller, 1996; Pekar et al., 2000). The upper Oligocene sequence O2 (348.02–344.71 rmcd) is dated with three Sr isotopic estimates of 24.4, 26.6, and 27.2 Ma. The median Sr age is 26.6 Ma, suggesting correlation with sequence O5 in New Jersey (Pekar and Miller, 1996; Pekar et al., 2000). An assumed sedimentation rate of 20 m/Ma results in an age for the sequence of 26.65–26.5 Ma.

Early and Middle Miocene Sequences

Early and middle Miocene sequences are correlated to sequences C4–C8 from Bethany Beach, Delaware. They are separated from the overlying V6 and younger sequences by a long hiatus (12.8–8.3 Ma; Fig. 9). The very thin basal Miocene sequence (344.71–344.34 rmcd) did not contain carbonate, and its age is constrained by dinocysts to DN2b (20–19.4 Ma). There are no sequences of equivalent age in the Bethany Beach borehole (Miller et al., 2003b). It is equivalent in age to the uppermost Kw1b sequence in New Jersey (Miller et al., 1997). Sequence V1 (344.34–337.63 rmcd) is dated with four Sr isotopic age estimates, which range from 18.1 to 18.4 Ma. An age of 15.6 Ma at 343.20 rmcd is presumed to be diagenetically altered. The median Sr age is 18.3 Ma. An assumed sedimentation rate of 50 m/Ma, typical for the early Miocene of this region (Browning et al., 2006), results in an age for the sequence of 18.4–18.2 Ma, which is at odds with the dinocyst data. The underlying sequence contains DN2b fossils, and the overlying sequence contains DN2c fossils (Table 4). Superposition and dinocyst biostratigraphy constrain this sequence to 20–19 Ma, which is older than the strontium dates. This suggests that either strontium is diagenetically altered or the dinocysts are miscalibrated to the geomagnetic polarity time scale (GPTS). Given this discrepancy, the sequence has an age uncertainty of 20–18.2 Ma.

The overlying sequence V2 (337.63–330.77 rmcd) is dated with four Sr isotopic ages ranging from 17.5 to 16.5 Ma, with a median Sr age of 17.0 Ma. The HO of *Catapsydrax unicava* in M3 at 334.06 rmcd provides a younger limit for the age of this sequence (17.3 Ma; Berggren et al., 1995). An assumed sedimentation rate of 50 m/Ma results in an age for the sequence of 17.4–17.3 Ma. Once again, this disagrees with the ages obtained from dinocyst data. Two samples 335.30 and 332.91 rmcd give ages of DN2c (19.4 and 19 Ma). The ages derived from strontium and dinocysts are incompatible, and the sequence may range in age from 19.4 Ma to 17.3 Ma. Nevertheless, the good agreement of Sr and highest occurrence of *Catapsydrax unicava* is suggestive of a time-scale calibration problem for dinocyst zone D2.

Sequence V3 (330.77–300.05 rmcd) is dated with nine Sr isotopic estimates ranging from 17.5 to 14.1 Ma. The data fall in two intermixed groups. Three data points range from 14.7 to 14.1 Ma, and the other six points range from 17.5 to 16.1 Ma. The older points are largely in agreement with dinocyst biostratigraphy (zone DN4 at 306.32 rmcd). The median of the Sr data gives an age of 16.2 Ma. An assumed sedimentation rate of 50 m/Ma results in a best estimate age for the sequence of 16.4–16.0 Ma. This result

agrees with the LO of *Praeorbulina sicana* (16.4 Ma; Berggren et al., 1995) at 329.61 rmcd, the LO of *Praeorbulina glomerosa curva* (found between 16.4 and 15.1 Ma; Kennett and Srinivasan, 1983) at 312.72 rmcd, and the LO of *Praeorbulina glomerosa glomerosa* (16.1 Ma; Berggren et al., 1995) at 305.13 rmcd. The strontium isotope data are also in agreement with five dinocyst age estimates of DN4 (16.7–15.1 Ma). The potential uncertainty in dating this sequence from the preferred estimate is that the base of the sequence could be as young as 15.4 Ma and the top of the sequence could be as young as 15.1 Ma.

Sequence V4 (300.05–248.63 rmcd) is dated with three Sr isotopic estimates ranging from 13.2 to 12.5 Ma and two dinocyst dates of zone DN5 (15.1–13.2 Ma; de Verteuil and Norris, 1996) at 288.07 and 263.48 rmcd. Only one Sr isotopic age is compatible with the dinocyst data. The best estimate age of the sequence is interpreted to be 14.8–14.1 Ma, which combines the oldest isotopic age and dinocyst biostratigraphy (Fig. 9). This is consistent with the presence of *Globorotalia praemenardii* (14.8–11.9 Ma; Kennett and Srinivasan, 1983; Berggren et al., 1995) at 263.87 rmcd. The uncertainty on the age of the base of the sequence is 15.3–14.4 Ma and the top of the sequence is 14.8–13.8 Ma.

Sequence V5 (248.53–207.13 rmcd) is dated with five Sr isotopic estimates that range from 14.1 to 10.7 Ma. Four dinocyst dates of zone DN5 between 228.97 and 219.67 rmcd are older than most of the Sr isotopic age estimates. In addition, there are two dinocyst ages of zone DN6 from the top of the sequence (214.27 and 208.31 rmcd). A best-fit line making the age-depth data fit the biostratigraphy and two of the strontium dates give a sequence age of 13.8–12.8 Ma and a sedimentation rate of 43 m/Ma. The uncertainty on the age of the base of the sequence is 14.8–13.8 Ma and the top of the sequence is 12.9–12.3 Ma.

Late Miocene and Younger Sequences

Interpreting age-depth plots for the section above 214.88 rmcd is especially difficult because of limited Sr isotope resolution due to the low rate of global change and the lack of biostratigraphic constraints (Fig. 10). Because of the scatter to the Sr isotope ages, it was not possible to use linear regression to estimate ages and sedimentation rates of the sequences. Sequence ages were assigned by determining the median for the Sr age estimates and fitting a sedimentation rate of ~50 m/Ma to the data for the V9, V10, and V11 sequences. This is similar to sedimentation rates found in the Bethany Beach core hole (Miller et al., 2003b; Browning et al., 2006) in similar facies. Sequences V6, V7, and V8 are thicker than the younger section, and higher sedimentation rates were needed to fit the available age data. For sequence V8, a sedimentation rate of ~80 m/Ma was applied to the data, and for sequences V7 and V6, a sedimentation rate of ~150 m/Ma was applied to the data.

The upper Miocene and Pliocene sequences are especially difficult to date with Sr isotopes because of the very large error bars associated with the low rate of change of Sr isotopes at this time.

The sequences V6, V7, and V8 are upper Miocene (Fig. 10). Sequence V6 is dated with six Sr isotopic ages. The interval con-

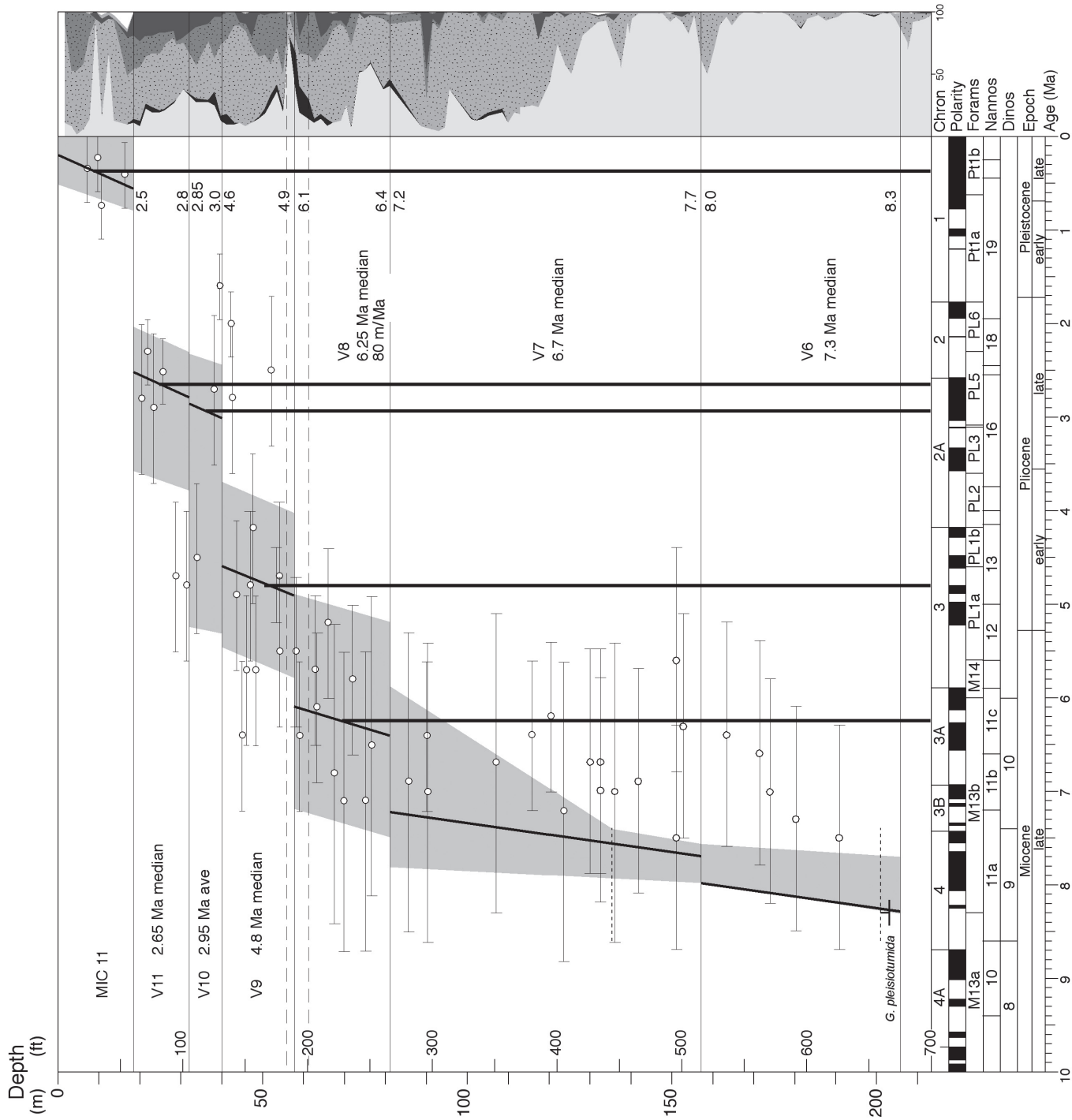


Figure 10. Age-depth plot showing the distribution through time of the upper Miocene through Pleistocene sequences in the Eyreville core hole. V6, V7, V8, V9, V10, V11, and MI C11 refer to sequences discussed in the text. Open circles are strontium age estimates with errors. Thin dashed lines are age estimates for dinocyst samples. Thin horizontal lines are inferred unconformities. Thick black lines between unconformities are the preferred age estimate. Shaded areas behind age estimates represent age uncertainties. Forams—planktonic foraminiferal zones; Nannos—calcareous nannoplankton zones; Dinos—dinoflagellate zones; G.—*Globorotalia*. Time scale is after Berggren et al. (1995). Key for lithology column is the same as for Figure 2. ave—average.

tained sparse calcite, and samples 175.60 and 172.49 rmcd had to be combined to get enough material for a Sr run. A seventh age of 18.3 Ma at 204.43 rmcd is assumed to be diagenetically altered. Two ages were obtained from mollusk shells, and they are much younger than the age estimates from foraminifers and are excluded from age estimates. The four ages form a cluster between 7.5 and 7.0 Ma. However, dinocyst picks of zone DN9 (8.6–7.4 Ma) at 202.55 rmcd and 135.39 rmcd in the overlying sequence are older than most of the Sr age estimates and help constrain the age of the V6 sequence. Assuming a 150 m/Ma sedimentation rate, the sequence was deposited between 8.3 and 8.0 Ma, but the base could be as young as 7.7 Ma, and the top of the sequence could be as young as 7.6 Ma. This is consistent with *Globorotalia pleisiotumida* (first appearance = 8.3 Ma, base M13b; Berggren et al., 1995) at 203.48 rmcd.

Fifteen Sr isotopic age estimates were obtained from sequence V7 (157.32–81.2 rmcd): eight from the Eyreville C hole and seven from the Eyreville A hole, and ages are from 7.5 to 6.2 Ma (Fig. 10). The sequence apparently had very high sedimentation rates. The median age of the Sr analyses is 6.7 Ma, younger than the age of zone DN9 identified in the lower part of the sequence (135.39 rmcd). The best estimate age of the sequence, making it fit the dinocyst age and as much of the strontium data as possible and assuming a sedimentation rate of 150 m/Ma, is 7.7–7.2 Ma. The uncertainty for the ages is 8.0–7.6 Ma at the base and 7.7–5.9 Ma for the top.

The age of sequence V8 (81.20–57.88 rmcd) is not constrained by biostratigraphic data. Sequence V8 has 10 Sr isotopic ages ranging from 6.8 to 5.6 Ma. The Sr ages generally increase upward within the sequence, but there is a great deal of scatter. The age of the sequence cannot be definitively determined. The median age of the Sr analyses is 6.25 Ma, and assuming an 80 m/Ma sedimentation rate, the sequence was deposited from 6.4 to 6.1 Ma. The uncertainty for the ages is 7.5–5.2 Ma at the base and 7.2–4.9 Ma for the top.

The V9 sequence (57.88–39.93 rmcd, lower Yorktown Formation) is dated with 11 Sr isotope estimates, and one other discordant sample was clearly affected by diagenesis (Fig. 10). Ages range from 6.4 to 2.0 Ma. This sequence is generally dated as Pliocene; however, the oldest Sr ages obtained at Eyreville are late Miocene. The median age of the Sr analyses is 4.8 Ma, and assuming a 50 m/Ma sedimentation rate, the sequence was deposited from 4.9 to 4.6 Ma. The uncertainty for the ages is 5.8–4.0 Ma at the base and 5.5–3.7 Ma for the top.

The upper Yorktown Formation has been dated elsewhere as ca. 2–3 Ma (Dowsett and Wiggs, 1992; Krantz, 1991). Three dates were obtained from the V10 sequence (39.93–32.16 rmcd): 1.6 Ma (39.75 rmcd), 4.5 Ma (33.99 rmcd), and 2.7 Ma (38.40 rmcd). Superposition likely constrains this sequence to older than 2.8 and younger than 4.6 Ma (Fig. 10). Assuming a 50 m/Ma sedimentation rate through the mean age, the sequence was deposited from ca. 3.0 to 2.8 Ma. The uncertainty for the ages is 5.3–2.4 Ma at the base and 5.2–2.3 Ma for the top.

We obtained six age estimates from sequence V11 (32.16–18.32 rmcd). A seventh sample (26.37 rmcd) yielded a Sr isotopic ratio not found in the Cenozoic and is interpreted to have been affected by diagenesis. Four samples yielded ages ranging from 2.9 to 2.3 Ma. Two samples from the bottom of the sequence gave ages of 4.8 and 4.7 Ma, but the Sr curves are very flat and error bars are very large for this interval. Previous studies (Dowsett and Wiggs, 1992) have found the age of this unit to be closer to the younger dates found here. Assuming the older dates are affected by diagenesis, the median age for the sequence is 2.65 Ma, and using a 50 m/Ma sedimentation rate, the sequence was deposited from 2.8 to 2.5 Ma. The uncertainty for the ages is 3.8–2.3 Ma at the base and 3.6–2.1 Ma for the top.

The uppermost sequence in the core (18.32–1.19 rmcd) yielded four Sr dates from shells ranging from 0.74 to 0.24 Ma. The median age for the data was 0.38 Ma. The timing of the Eyreville sequence is similar to marine isotope chron 11 (spans from 420 to 360 ka), and we tentatively correlate the sequence here to marine isotope chron 11.

DISCUSSION

Previous studies have documented the mid-Atlantic margin as an excellent natural laboratory to study of the effects of sea-level changes on sedimentation patterns (Miller et al., 2005). As a passive margin, creation of accommodation space is generally dominated by thermoflexural subsidence and eustasy (Kominz et al., 1998; Kominz and Pekar, 2001). There is little evidence for more active tectonism in the New Jersey and Delaware region (Kominz et al., 1998; Kominz and Pekar, 2001; Miller et al., 2005) other than minor (tens of meters) regional uplift or subsidence (Browning et al., 2006). Active faulting has occurred in the Atlantic Coastal Plain south of the Salisbury Embayment (e.g., near Charleston, South Carolina; Weems and Lewis, 2002), and active faults may be present on the south side of the Salisbury Embayment as an aftermath of the Chesapeake Bay impact structure (Johnson et al., 1998; Poag et al., 2004; Kulpecz et al., this volume). However, other evidence for major Miocene faulting in the New Jersey coastal plain is equivocal; this region lacks evidence for the large number or magnitude of earthquakes found elsewhere in the Atlantic Coastal Plain (Seeber and Armbruster, 1988). Sea-level change has been shown to be the dominant signal in New Jersey and Delaware middle Miocene sequences (Miller et al., 2005).

Accommodation from thermoflexural subsidence is overprinted by sea-level changes that allow the deposition and preservation of unconformity-bounded sequences. The degree to which sea level dominates sedimentation patterns within the Chesapeake Bay impact structure over other processes, such as tectonics and sediment-supply changes, is an important question. Numerous faults active in the past 35 Ma are recognized in the area near the Chesapeake Bay impact structure and have influenced sedimentation patterns (Poag, 1997; Powars and Bruce, 1999).

Early to middle Miocene sequences from the Chesapeake Bay impact structure show a close correspondence in number and timing to sequences from New Jersey core holes and the Bethany Beach, Delaware, core hole. The three Eyreville sequences deposited between 16.4 and 12.8 Ma (Table 3) correspond to sequences C6, C7, and C8 of Browning et al. (2006) in the Bethany Beach core hole and to sequences Kw2b, Kw2c, and Kw3 of Miller et al. (1997), respectively (Fig. 11). Sequences V1 and V2 in the Eyreville core hole may correlate with sequences C4 and C5 of Browning et al. (2006) in the Bethany Beach core hole and to sequences Kw1c and Kw2a of Miller et al. (1997), if strontium ages are correct; however, sequence V1 at Eyreville might correlate with sequence Kw1b in New Jersey and sequence V2 at Eyreville might correlate with sequences C2 from Bethany Beach and Kw1c from New Jersey if the dinocyst correlations are correct.

As shown herein, the three regions differ markedly in the kinds of sedimentary environments represented, yet they show a similar pattern in the early to middle Miocene (Fig. 11). Sedimentation in New Jersey at this time was heavily influenced by large river deltas bringing sediment to the coast, and Bethany Beach was a storm-dominated coastline with nearshore deposits. Sediments at Eyreville were deposited in much deeper neritic (generally middle neritic) environments compared to the New Jersey or Delaware sections. The close timing of sequence boundaries in widely separated areas with different sedimentological settings suggests a common cause, in this case, eustatic change.

Changes in oxygen isotopes of deep-sea benthic foraminifers are used as a proxy for global sea-level change, particularly in times, such as the early Miocene, when there is known to be a large volume of ice on Antarctica (Miller et al., 1991; Williams and Handwerger, 2005). Although changes in oxygen isotopes reflect both changes in bottom water temperature as well as ice volume, at least half of the Miocene oxygen isotope signal is thought to reflect ice-volume changes in the Miocene (e.g., Miller et al., 1991). Several large increases in oxygen isotope values in the early to mid-Miocene have been identified and associated with ice-volume growth (Miller et al., 1991, 1998; Wright and Miller, 1992; Zachos et al., 1992). Sequence boundaries at the bases of sequences V1, V2, V3, V4, and V5 correspond to oxygen isotope events Mi1b (Mi1a dinocysts), an unnamed event at ca. 17.5 Ma (Mi1ab? dinocysts), Mi2, Mi2a?, and Mi3a and Mi3b, respectively (Fig. 11). This close correspondence between the global proxy for sea level and the sequence boundaries from the middle Atlantic Coastal Plain (Fig. 11) suggests that global sea level was the dominant factor influencing the formation of sequence boundaries on this passive margin, and it provides a template of available sequences that can be deposited.

Late late Miocene and Pliocene sequences (i.e., from ca. 8 to 2 Ma) have not been dated in either New Jersey or Delaware. Thus, the upper sequences at Eyreville allow a first correlation of the timing of sequence boundaries on the Atlantic margin with the oxygen isotopic proxy for sea level. Major oxygen isotopic inflections from the late Miocene and Pliocene were identified

by Miller et al. (2005) and are shown as red lines on Figure 11. Inferred ice-growth events at ca. 9.5 Ma (= Mi7; Wright and Miller, 1992) and at 8.2 Ma correlate with the hiatus beneath the V6 sequence (12.8–8.3 Ma). No major ice-growth events were identified by Miller et al. (2005) that would correlate with the sequence boundaries beneath the V7 sequence (hiatus 8.0–7.7 Ma) or the V8 sequence (hiatus 7.2–6.4 Ma; Fig. 11). The oxygen isotopic curve is relatively flat in this time interval, although these sequence boundaries may represent smaller ice-growth events more difficult to resolve in an oxygen isotopic record. We note that there is a possible million-year-scale $\delta^{18}\text{O}$ increase at ca. 7.2 Ma that appears to correlate with the base of V7 (shown as a dashed line on Fig. 11); Westerhold et al. (2005) also reported a similar sea-level fall at this time.

The sequence boundary at the base of sequence V9 (hiatus 6.1–4.9 Ma) correlates with isotopic inflections at 5.7 and 4.9 Ma and also corresponds with the Messinian salinity crisis (5.96 Ma; Ryan, et al., 1974). Similarly, sequence V10 (hiatus 4.6–3 Ma) encompasses both the 4.0 and 3.3 Ma million-year-scale $\delta^{18}\text{O}$ increases. Although no isotopic inflection was identified with the sequence boundary at the base of sequence V11 (hiatus 2.85–2.8 Ma), this is very likely correlative to the 2.5 Ma event (now dated as 2.6 Ma) associated with an increased scale of glaciation in the Northern Hemisphere (Shackleton et al., 1984). The two Pleistocene sequences are tentatively correlated with the peaks in sea level during marine isotope chron 11 and possibly 5e.

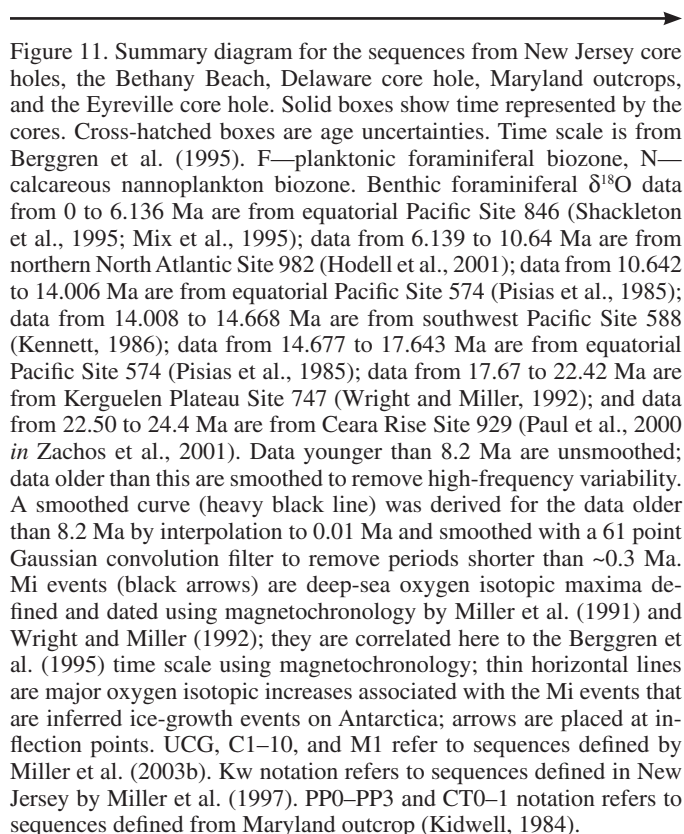
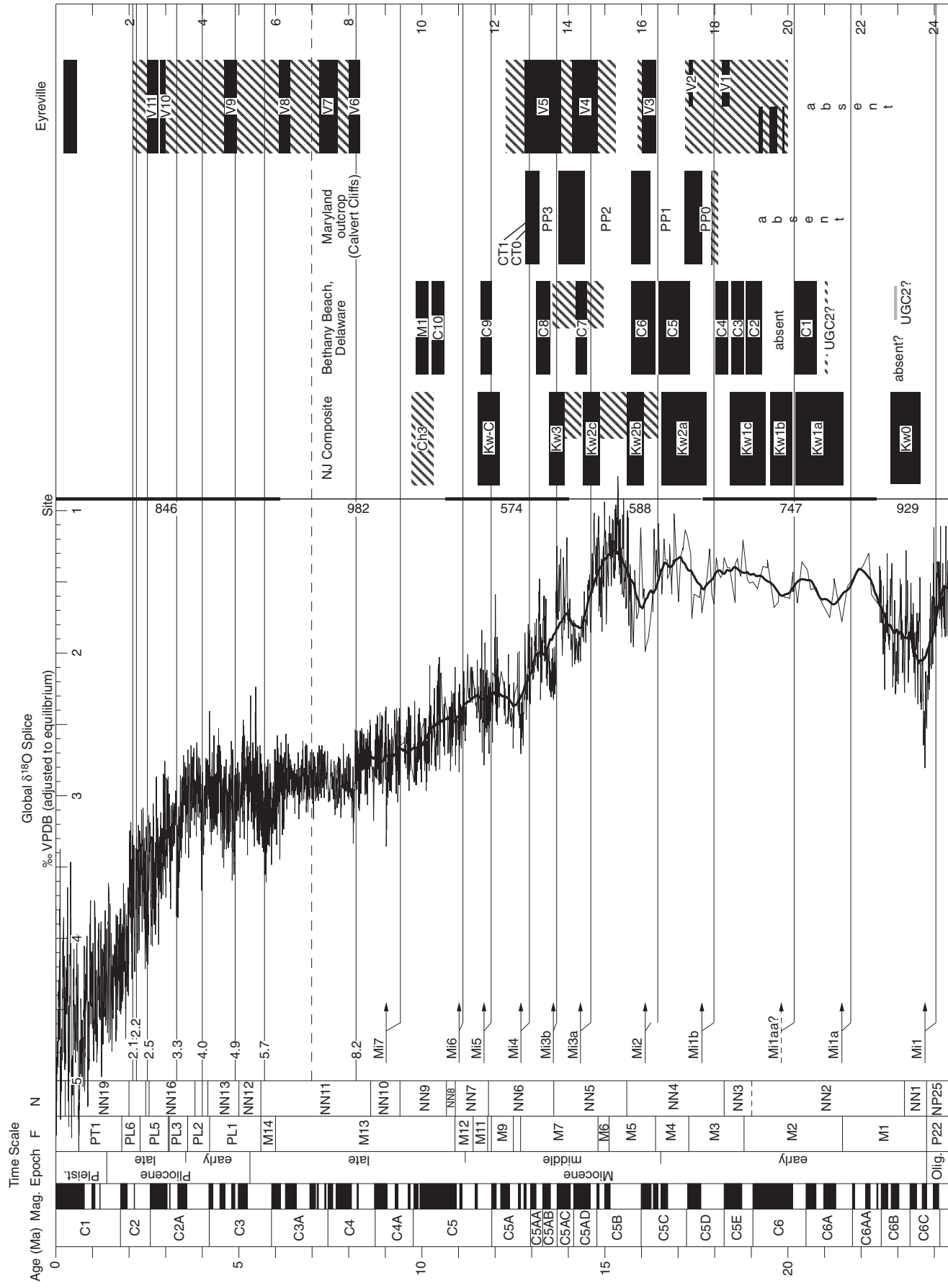


Figure 11. Summary diagram for the sequences from New Jersey core holes, the Bethany Beach, Delaware core hole, Maryland outcrops, and the Eyreville core hole. Solid boxes show time represented by the cores. Cross-hatched boxes are age uncertainties. Time scale is from Berggren et al. (1995). F—planktonic foraminiferal biozone, N—calcareous nannoplankton biozone. Benthic foraminiferal $\delta^{18}\text{O}$ data from 0 to 6.136 Ma are from equatorial Pacific Site 846 (Shackleton et al., 1995; Mix et al., 1995); data from 6.139 to 10.64 Ma are from northern North Atlantic Site 982 (Hodell et al., 2001); data from 10.642 to 14.006 Ma are from equatorial Pacific Site 574 (Pisias et al., 1985); data from 14.008 to 14.668 Ma are from southwest Pacific Site 588 (Kennett, 1986); data from 14.677 to 17.643 Ma are from equatorial Pacific Site 574 (Pisias et al., 1985); data from 17.67 to 22.42 Ma are from Kerguelen Plateau Site 747 (Wright and Miller, 1992); and data from 22.50 to 24.4 Ma are from Ceara Rise Site 929 (Paul et al., 2000 in Zachos et al., 2001). Data younger than 8.2 Ma are unsmoothed; data older than this are smoothed to remove high-frequency variability. A smoothed curve (heavy black line) was derived for the data older than 8.2 Ma by interpolation to 0.01 Ma and smoothed with a 61 point Gaussian convolution filter to remove periods shorter than ~0.3 Ma. Mi events (black arrows) are deep-sea oxygen isotopic maxima defined and dated using magnetostratigraphy by Miller et al. (1991) and Wright and Miller (1992); they are correlated here to the Berggren et al. (1995) time scale using magnetostratigraphy; thin horizontal lines are major oxygen isotopic increases associated with the Mi events that are inferred ice-growth events on Antarctica; arrows are placed at inflection points. UCG, C1–10, and M1 refer to sequences defined by Miller et al. (2003b). Kw notation refers to sequences defined in New Jersey by Miller et al. (1997). PP0–PP3 and CT0–1 notation refers to sequences defined from Maryland outcrop (Kidwell, 1984).



CONCLUSIONS

The Eyreville core holes were very successful in recovering a postimpact record of sequences. Most of the sequence boundaries, particularly in the early to middle Miocene, can be correlated with previously recognized sequences in New Jersey and Delaware and with the oxygen isotopic proxy for sea level, confirming that, in the absence of active tectonics on a passive margin, eustatic changes driven by ice-volume changes can provide a template for available sequences. The late Miocene to Pliocene chronology of sequences from the Eyreville cores is presented here for the first time. Although this record needs verification in other core holes, we show that the timing of most sequence boundaries correlates with inferred sea-level decreases from ice-volume increases. Differences among the packages of sediment exist. For example, there are long hiatuses at Eyreville from ca. 26 to ca. 20 Ma and from ca. 13 to 8.3 Ma that must be ascribed to nonthermal tectonism (see Kulpecz et al. [this volume] for a discussion of the causes of these differences).

ACKNOWLEDGMENTS

We thank Peter Schulte and Kelvin Ramsey for reviews; G. Gohn, C. Koeberl, and U. Reimold for planning drilling at Eyreville; the U.S. Geological Survey (USGS) for logging the hole; the entire USGS, Rutgers, and international team that worked this site; P. Sugarman for helpful discussions; J. Self-Trail for Eocene calcareous nannoplankton zonation; C. Wylie Poag for discussions of the paleoenvironment of the Chickahominy Formation; DOSECC (Drilling, Observing and Sampling of the Earth's Continental Crust) for contracting the drilling; G. Cobb III (USGS) for drilling hole C; Major Drilling for drilling hole A; and the Buyn family for providing access to the site. This work was supported by National Science Foundation grants EAR-0506720 and EAR-0606693 (to Miller, Browning, and Kominz).

REFERENCES CITED

- Berggren, W.A., and Pearson, P.N., 2005, A revised tropical to subtropical Paleogene planktonic foraminiferal zonation: *Journal of Foraminiferal Research*, v. 35, p. 279–298, doi: 10.2113/35.4.279.
- Berggren, W.A., Kent, D.V., Swisher, C.C., III, and Aubry, M.-P., 1995, A revised Cenozoic geochronology and chronostratigraphy, in Berggren, W.A., Kent, D.V., Aubry, M.-P., and Hardenbol, J., eds., *Geochronology, Time Scales and Global Stratigraphic Correlations: A Unified Temporal Framework for an Historical Geology*: Society for Sedimentary Geology Special Publication 54, p. 129–212.
- Bernard, H.A., Le Blanc, J.R.J., and Major, C.F., 1962, Recent and Pleistocene geology of southeast Texas, in Rainwater, E.H., and Zingula, R.P., eds., *Geology of the Gulf Coast and Central Texas and Guidebook of Excursions*: Houston, Houston Geological Society, p. 175–224.
- Browning, J.V., Miller, K.G., McLaughlin, P.P., Kominz, M.A., Sugarman, P.J., Monteverde, D., Feigenson, M.D., and Hernández, J.C., 2006, Quantification of the effects of eustasy, subsidence, and sediment supply on Miocene sequences, Mid-Atlantic margin of the United States: *Geological Society of America Bulletin*, v. 118, p. 567–588, doi: 10.1130/B25551.1.
- Browning, J.V., Miller, K.G., Sugarman, P.J., Kominz, M.A., McLaughlin, P.P., and Kulpecz, A.A., 2008, 100 Myr record of sequences, sedimentary facies and sea-level change from Ocean Drilling Program onshore core-holes, U.S. Mid-Atlantic coastal plain: *Basin Research*, v. 20, p. 227–248, doi: 10.1111/j.1365-2117.2008.00360.x.
- de Verteuil, L., and Norris, G., 1996, Miocene dinoflagellate stratigraphy and systematics of Maryland and Virginia: *Micropaleontology*, v. 42, suppl., p. 1–172.
- Dowsett, H.J., and Wiggs, L.B., 1992, Planktonic foraminiferal assemblage of the Yorktown Formation, Virginia, USA: *Micropaleontology*, v. 38, p. 75–86, doi: 10.2307/1485844.
- Edwards, L.E., Powars, D.S., Browning, J.V., McLaughlin, P.P., Jr., Miller, K.G., Self-Trail, J.M., Kulpecz, A.A., and Elbra, T., 2009, this volume, Geologic columns for the ICDP-USGS Eyreville A and C cores, Chesapeake Bay impact structure: Postimpact sediments, 444 to 0 m depth, in Gohn, G.S., Koeberl, C., Miller, K.G., and Reimold, W.U., eds., *The ICDP-USGS Deep Drilling Project in the Chesapeake Bay Impact Structure: Results from the Eyreville Core Holes*: Geological Society of America Special Paper 458, doi: 10.1130/2009.2458(04).
- Farrell, J.W., Clemens, S., and Gromet, L.P., 1995, Improved chronostratigraphic reference curve of late Neogene seawater: $^{87}\text{Sr}/^{86}\text{Sr}$: *Geology*, v. 23, p. 403–406, doi: 10.1130/0091-7613(1995)023<0403:ICRCOL>2.3.CO;2.
- Harms, J.C., Southard, J.B., Spearing, D.R., and Walker, R.G., 1975, Depositional Environments as Interpreted from Primary Sedimentary Structures and Stratification Sequences: Lecture Notes for Short Course 2: Dallas, Texas, Society of Economic Paleontologists and Mineralogists, 161 p.
- Harms, J.C., Southard, J.B., and Walker, R.G., 1982, Structure and Sequence in Clastic Rocks: Lecture Notes for Short Course 9: Tulsa, Oklahoma, Society of Economic Paleontologists and Mineralogists, 249 p.
- Hart, S.R., and Brooks, C., 1974, Clinopyroxene-matrix partitioning of K, Rb, Cs, and Ba: *Geochimica et Cosmochimica Acta*, v. 38, p. 1799–1806, doi: 10.1016/0016-7037(74)90163-X.
- Hayden, T., Kominz, M., Powars, D.S., Edwards, L.E., Miller, K.G., Browning, J.V., and Kulpecz, A.A., 2008, Impact effects and regional tectonic insights: Backstripping the Chesapeake Bay impact structure: *Geology*, v. 36, p. 327–330, doi: 10.1130/G24408A.1.
- Hodell, D.A., Curtis, J.H., Sierro, F.J., and Raymo, M.E., 2001, Correlation of late Miocene to early Pliocene sequences between the Mediterranean and North Atlantic: *Paleoceanography*, v. 16, p. 164–178, doi: 10.1029/1999PA000487.
- Johnson, G.H., Kruse, S.E., Vaughn, A.W., Lucey, J.K., Hobbs, C.H., and Powars, D.S., 1998, Postimpact deformation associated with the late Eocene Chesapeake Bay impact structure in southeastern Virginia: *Geology*, v. 26, p. 507–510, doi: 10.1130/0091-7613(1998)026<0507:PDATWL>2.3.CO;2.
- Kennett, J.P., 1986, Miocene to early Pliocene oxygen and carbon isotope stratigraphy in the southwest Pacific, Deep Sea Drilling Project Leg 90: Initial Reports of the Deep Sea Drilling Project, Volume 90: Washington, D.C., U.S. Government Printing Office, p. 1383–1411, doi: 10.2973/dsdp.proc.90.1986.
- Kennett, J.P., and Srinivasan, S., 1983, *Neogene Planktonic Foraminifer: A Phylogenetic Atlas*: Stroudsburg, Pennsylvania, Hutchinson Ross Publishing Company, 265 p.
- Kidwell, S.M., 1984, Outcrop features and origin of the basin margin unconformities in the lower Chesapeake group (Miocene), Atlantic Coastal Plain, in Schlee, J.S., ed., *Interregional Unconformities and Hydrocarbon Accumulation*: American Association of Petroleum Geologists Memoir 36, p. 37–58.
- Koeberl, C., Poag, C.W., Reimold, W.U., and Brandt, D., 1996, Impact origin of Chesapeake Bay structure and the source for the North American tektites: *Science*, v. 271, p. 1263–1266, doi: 10.1126/science.271.5253.1263.
- Kominz, M.A., and Pekar, S.F., 2001, Oligocene eustasy from two-dimensional sequence stratigraphic backstripping: *Geological Society of America Bulletin*, v. 113, p. 291–314, doi: 10.1130/0016-7606(2001)113<0291:OEFTDS>2.0.CO;2.
- Kominz, M.A., Miller, K.G., and Browning, J.V., 1998, Long-term and short-term global Cenozoic sea-level estimates: *Geology*, v. 26, p. 311–314, doi: 10.1130/0091-7613(1998)026<0311:LTASTG>2.3.CO;2.
- Kominz, M.A., Van Sickel, W.A., Miller, K.G., Browning, J.V., Misintseva, S., and Scotese, C.R., 2008, Late Cretaceous to Miocene sea-level estimates from the New Jersey and Delaware coastal plain coreholes: An error analysis: *Basin Research*, v. 20, p. 211–226, doi: 10.1111/j.1365-2117.2008.00354.x.
- Krantz, D.E., 1991, A chronology of Pliocene sea-level fluctuations: The U.S. middle Atlantic Coastal Plain record: *Quaternary Science Reviews*, v. 10, p. 163–174, doi: 10.1016/0277-3791(91)90016-N.

- Kulpecz, A.A., Miller, K.G., Browning, J.V., Edwards, L.E., Powars, D.S., McLaughlin, P.P., Jr., Harris, A.D., and Feigenson, M.D., 2009, this volume, Postimpact deposition in the Chesapeake Bay impact structure: Variations in eustasy, compaction, sediment supply, and passive-aggressive tectonism, *in* Gohn, G.S., Koeberl, C., Miller, K.G., and Reimold, W.U., eds., The ICDP-USGS Deep Drilling Project in the Chesapeake Bay Impact Structure: Results from the Eyreville Core Holes: Geological Society of America Special Paper 458, doi: 10.1130/2009.2458(34).
- Martin, E.E., Shackleton, N.J., Zachos, J.C., and Flower, B.P., 1999, Orbitally-tuned Sr isotope chemostratigraphy for the late middle to late Miocene: *Paleoceanography*, v. 14, p. 74–83, doi: 10.1029/1998PA000008.
- McArthur, J.M., Howarth, R.J., and Bailey, T.R., 2001, Strontium isotope stratigraphy: LOWESS version 3. Best-fit line to the marine Sr-isotope curve for 0 to 509 Ma and accompanying look-up table for deriving numerical age (look-up table version 4: 08/03): *The Journal of Geology*, v. 109, p. 155–169, doi: 10.1086/319243.
- McCubbin, D.G., 1982, Barrier-island and strand plain facies, *in* Scholle, P.A., and Spearing, D., eds., Sandstone Depositional Environments: American Association of Petroleum Geologists Memoir 31, p. 247–279.
- Miller, K.G., and Mountain, G.S., 1994, Global sea-level change and the New Jersey margin, *in* Mountain, G.S., Miller, K.G., Blum, P., et al., Proceedings of the Ocean Drilling Program, Initial Reports, Volume 150: College Station, Texas, Ocean Drilling Program, p. 11–20.
- Miller, K.G., Wright, J.D., and Fairbanks, R.G., 1991, Unlocking the ice house: Oligocene-Miocene oxygen isotopes, eustasy, and margin erosion: *Journal of Geophysical Research*, v. 96, p. 6829–6848, doi: 10.1029/90JB02015.
- Miller, K.G., Mountain, G.S., the Leg 150 Shipboard Party, and Members of the New Jersey Coastal Plain Drilling Project, 1996, Drilling and dating New Jersey Oligocene-Miocene sequences: Ice volume, global sea level, and Exxon records: *Science*, v. 271, p. 1092–1094.
- Miller, K.G., Rufolo, S., Sugarman, P.J., Pekar, S.F., Browning, J.V., and Gwynn, D.W., 1997, Early to middle Miocene sequences, systems tracts, and benthic foraminiferal biofacies, New Jersey coastal plain, *in* Miller, K.G., Snyder, S.W., et al., Proceedings of the Ocean Drilling Program, Scientific Results, Volume 150X: College Station, Texas, Ocean Drilling Program, p. 169–186.
- Miller, K.G., Mountain, G.S., Browning, J.V., Kominz, M.A., Sugarman, P.J., Christie-Blick, N., Katz, M.E., and Wright, J.D., 1998, Cenozoic global sea-level, sequences, and the New Jersey transect: Results from coastal plain and slope drilling: *Reviews of Geophysics*, v. 36, p. 569–601, doi: 10.1029/98RG01624.
- Miller, K.G., Browning, J.V., Sugarman, P.J., McLaughlin, P.P., Kominz, M.A., Olsson, R.K., Wright, J.D., Cramer, B.S., Pekar, S.J., and Van Sickle, W., 2003a, 174AX Leg summary: Sequences, sea level, tectonics, and aquifer resources: Coastal plain drilling, *in* Miller, K.G., Sugarman, P.J., Browning, J.V., et al., Proceedings of the Ocean Drilling Program, Initial Reports, Volume 174AX (Suppl.): College Station, Texas, Ocean Drilling Program, p. 1–38.
- Miller, K.G., McLaughlin, P.P., Browning, J.V., Benson, R.N., Sugarman, P.J., Hernandez, J., Ramsey, K.W., Baxter, S.J., Feigenson, M.D., Aubry, M.-P., Monteverde, D.H., Cramer, B.S., Katz, M.E., McKenna, T.E., Strohmeier, S.A., Pekar, S.F., Uptegrove, J., Cobbs, G., Cobbs, G., III, and Curtin, S.E., 2003b, Bethany Beach site, *in* Miller, K.G., Sugarman, P.J., Browning, J.V., et al., Proceedings of the Ocean Drilling Program, Initial Reports, Volume 174AX (Suppl.): College Station, Texas, Ocean Drilling Program, p. 1–84.
- Miller, K.G., Sugarman, P.J., Browning, J.V., Kominz, M.A., Olsson, R.K., Feigenson, M.D., and Hernández, J.C., 2004, Upper Cretaceous sequences and sea-level history, New Jersey coastal plain: *Geological Society of America Bulletin*, v. 116, p. 368–393, doi: 10.1130/B25279.1.
- Miller, K.G., Kominz, M.A., Browning, J.V., Wright, J.D., Mountain, G.S., Katz, M.E., Sugarman, P.J., Cramer, B.S., Christie-Blick, N., and Pekar, S.F., 2005, The Phanerozoic record of global sea-level change: *Science*, v. 310, p. 1293–1298, doi: 10.1126/science.1116412.
- Miller, K.G., Sugarman, P.J., Browning, J.V., Aubry, M.-P., Brenner, G.J., Cobbs, G., III, de Romero, L., Feigenson, M.D., Harris, A., Katz, M.E., Kulpecz, A., McLaughlin, P.P., Jr., Misintseva, S., Monteverde, D.H., Olsson, R.K., Patrick, L., Pekar, S.J., and Uptegrove, J., 2006, Sea Girt site, *in* Miller, K.G., Sugarman, P.J., Browning, J.V., et al., Proceedings of the Ocean Drilling Program, Initial Reports, Volume 174AX (Suppl.): College Station, Texas, Ocean Drilling Program, p. 1–104.
- Mitchum, R.M., Vail, P.R., and Thompson, S., 1977, The depositional sequence as a basic unit for stratigraphic analysis, *in* Payton, C.E., ed., *Seismic Stratigraphy—Applications to Hydrocarbon Exploration*: American Association of Petroleum Geologists Memoir 26, p. 53–62.
- Mix, A.C., Le, J., and Shackleton, N.J., 1995, Benthic foraminiferal stable isotope stratigraphy of Site 846: 0–1.8 Ma: *Proceedings of the Ocean Drilling Program, Scientific Results, Volume 138*: College Station, Texas, Ocean Drilling Program, p. 839–854.
- Ormö, J., and Lindström, M., 2000, When a cosmic impact strikes the seabed: *Geological Magazine*, v. 137, p. 67–80, doi: 10.1017/S0016756800003538.
- Oslick, J.S., Miller, K.G., Feigenson, M.D., and Wright, J.D., 1994, Oligocene-Miocene strontium isotopes: Stratigraphic revisions and correlations to an inferred glaciostatic record: *Paleoceanography*, v. 9, p. 427–443, doi: 10.1029/94PA00249.
- Owens, J.P., and Sohl, N.F., 1969, Shelf and deltaic paleoenvironments in the Cretaceous-Tertiary formations of the New Jersey coastal plain, *in* Subitzky, S., ed., *Geology of Selected Areas in New Jersey and Eastern Pennsylvania and Guidebook of Excursions*: New Brunswick, New Jersey, Rutgers University Press, p. 390–408.
- Paul, H.A., Zachos, J.C., Flower, B.P., and Tripati, A., 2000, Orbitally induced climate and geochemical variability across the Oligocene/Miocene boundary: *Paleoceanography*, v. 15, p. 471–485, doi: 10.1029/1999PA000443.
- Pekar, S.F., and Miller, K.G., 1996, New Jersey Oligocene “icehouse” sequences (ODP Leg 150X) correlated with global $\delta^{18}\text{O}$ and Exxon eustatic records: *Geology*, v. 24, p. 567–570, doi: 10.1130/0091-7613(1996)024<0567:NJOISO>2.3.CO;2.
- Pekar, S.F., Miller, K.G., and Kominz, M.A., 2000, Reconstructing the stratal geometry of latest Eocene to Oligocene sequences in New Jersey: Resolving a patchwork distribution into a clear pattern of progradation: *Sedimentary Geology*, v. 134, p. 93–109, doi: 10.1016/S0037-0738(00)00015-4.
- Pekar, S.F., Christie-Blick, N., Kominz, M.A., and Miller, K.G., 2002, Calibration between eustatic estimates from backstripping and oxygen isotopic records for the Oligocene: *Geology*, v. 30, p. 903–906, doi: 10.1130/0091-7613(2002)030<0903:CBEEFB>2.0.CO;2.
- Pisias, N.G., Shackleton, N.J., and Hall, M.A., 1985, Stable isotope and calcium carbonate records from hydraulic piston cored Hole 574A: High-resolution records from the middle Miocene, *in* Mayer, L., Theyer, F., et al., Initial Reports of the Deep Sea Drilling Project, Volume 85: Washington, D.C., U.S. Government Printing Office, p. 735–748.
- Poag, C.W., 1997, The Chesapeake Bay bolide impact: A convulsive event in Atlantic Coastal Plain evolution: *Sedimentary Geology*, v. 108, p. 45–90, doi: 10.1016/S0037-0738(96)00048-6.
- Poag, C.W., 2009, this volume, Paleoenvironmental recovery from the Chesapeake Bay bolide impact: The benthic foraminiferal record, *in* Gohn, G.S., Koeberl, C., Miller, K.G., and Reimold, W.U., eds., The ICDP-USGS Deep Drilling Project in the Chesapeake Bay Impact Structure: Results from the Eyreville Core Holes: Geological Society of America Special Paper 458, doi: 10.1130/2009.2458(32).
- Poag, C.W., and Commeau, J.A., 1995, Paleocene to middle Miocene planktic foraminifera of the southwestern Salisbury Embayment, Virginia and Maryland: biostratigraphy, allostratigraphy, and sequence stratigraphy: *Journal of Foraminiferal Research*, v. 25, p. 134–155.
- Poag, C.W., Powars, D.S., Poppe, L.J., and Mixon, R.B., 1994, Meteoroid mayhem in Ole Virginny—Source of the North American tektite strewn field: *Geology*, v. 22, p. 691–694, doi: 10.1130/0091-7613(1994)022<0691:MMIOVS>2.3.CO;2.
- Poag, C.W., Koeberl, C., and Reimold, W.U., 2004, The Chesapeake Bay Crater: Geology and Geophysics of a Late Eocene Submarine Impact Structure: New York, Springer-Verlag, 522 p.
- Posamentier, H.W., Jervey, M.T., and Vail, P.R., 1988, Eustatic controls on clastic deposition I—Conceptual framework, *in* Wilgus, C.K., Hastings, B.S., Ross, C.A., Posamentier, H.W., Van Wagoner, J.C., and Kendall, C.G.St.C., eds., *Sea Level Changes: An Integrated Approach*: Society of Economic Paleontologists and Mineralogists Special Publication 42, p. 109–124.
- Powars, D.S., and Bruce, T.S., 1999, The Effects of the Chesapeake Bay Impact Crater on the Geologic Framework and the Correlation of Hydrogeologic Units of Southeastern Virginia, South of the James River: U.S. Geological Survey Professional Paper 1612, p. 82 p.
- Powars, D.S., Poag, C.W., and Mixon, R.B., 1993, The Chesapeake Bay “impact crater”—Stratigraphic and seismic evidence: *Geological Society of America Abstracts with Programs*, 25, no. 6, p. A-378.
- Powars, D.S., Bruce, T.S., Edwards, L.E., Gohn, G.S., Self-Trail, J.M., Weems, R.E., Johnson, G.H., Smith, J.J., and McCartan, C.T., 2005, Physical stratigraphy of the upper Eocene to Quaternary postimpact section in the

- USGS-NASA Langley corehole, Hampton, Virginia, chapter G, in Horton, J.W., Jr., Powars, D.S., and Gohn, G.S., eds., *Studies of the Chesapeake Bay Impact Structure—The USGS-NASA Langley Corehole, Hampton, Virginia, and Related Coreholes and Geophysical Surveys: U.S. Geological Survey Professional Paper 1688*, p. G1–G44.
- Pusz, A.E., Miller, K.G., Wright, J.D., Katz, M.E., Cramer, B.S., and Kent, D.V., 2009, Stable isotopic response to late Eocene extraterrestrial impacts, in Koeberl, C., and Montanari, A., eds., *The Late Eocene Earth—Hothouse, Icehouse, and Impacts: Geological Society of America Special Paper 452*, p. 83–96.
- Ryan, W.B.E., Cita, M.B., Dreyfus Rawson, M., Burckle, L.H., and Saito, T., 1974, A paleomagnetic assignment of Neogene stage boundaries and the development of isochronous datum planes between the Mediterranean, the Pacific and the Indian Oceans in order to investigate the response of the world oceans to the Mediterranean “salinity crisis”: *Rivista Italiana di Paleontologia e Stratigrafia*, v. 80, p. 631–688.
- Sanford, W.E., Gohn, G.S., Powars, D.S., Horton, J.W., Jr., Edwards, L.E., Self-Trail, J.M., and Morin, R.H., 2004, Drilling the central crater of the Chesapeake Bay impact structure: A first look: *Eos (Transactions, American Geophysical Union)*, v. 85, p. 369, 377.
- Schulte, P., Wade, B.S., Kontny, A., and Self-Trail, J.M., 2009, this volume, The Eocene-Oligocene sedimentary record in the Chesapeake Bay impact structure: Implications for climate and sea-level changes on the Western Atlantic margin, in Gohn, G.S., Koeberl, C., Miller, K.G., and Reimold, W.U., eds., *The ICDP-USGS Deep Drilling Project in the Chesapeake Bay Impact Structure: Results from the Eyreville Core Holes: Geological Society of America Special Paper 458*, doi: 10.1130/2009.2458(35).
- Seeber, L., and Armbruster, J.G., 1988, Seismicity along the Atlantic seaboard of the U.S.: Intraplate neotectonics and earthquake, in Sheridan, R.E., and Grow, J.A., eds., *The Atlantic Continental Margin, U.S.: Boulder, Colorado, Geological Society of America, Geology of North America*, v. I-2, p. 437–444.
- Shackleton, N.J., Backman, J., Zimmerman, H., Kent, D.V., Hall, M.A., Roberts, D.G., Schnitker, D., Baldauf, J.G., Desprairies, A., Homrighausen, R., Huddleston, P., Keene, J.B., Kaltenback, A.J., Krumstiek, K.A.D., Morton, A.C., Murray, J.W., and Westberg-Smith, J., 1984, Oxygen isotope calibration of the onset of ice-rafting and history of glaciation in the northeast Atlantic: *Nature*, v. 307, p. 620–623, doi: 10.1038/307620a0.
- Shackleton, N.J., Hall, M.A., and Pate, D., 1995, Pliocene stable isotope stratigraphy of Site 846, in Pisias, N.G., Mayer, L.A., Janecek, T.R., Palmer-Julson, A., van Andel, T.H., et al., *Proceedings of the Ocean Drilling Program, Scientific Results, Volume 138: College Station, Texas, Ocean Drilling Program*, p. 337–353.
- Sugarman, P.J., Miller, K.G., Owens, J.P., and Feigenson, M.D., 1993, Strontium isotope and sequence stratigraphy of the Miocene Kirkwood Formation, southern New Jersey: *Geological Society of America Bulletin*, v. 105, p. 423–436, doi: 10.1130/0016-7606(1993)105<0423:SIASSO>2.3.CO;2.
- Sugarman, P.J., Miller, K.G., Bukry, D., and Feigenson, M.D., 1995, Uppermost Campanian-Maestrichtian strontium isotopic, biostratigraphic, and sequence stratigraphic framework of the New Jersey Coastal Plain: *Geological Society of America Bulletin*, v. 107, p. 19–37, doi: 10.1130/0016-7606(1995)107<0019:UCMSIB>2.3.CO;2.
- Watts, A.B., and Steckler, M.S., 1979, Subsidence and eustasy at the continental margin of eastern North America, in Talwani, M., Hay, W., and Ryan, W.B.F., eds., *Deep Drilling Results in the Atlantic Ocean: Continental Margins and Paleoenvironment: Washington, D.C., American Geophysical Union Maurice Ewing Series*, v. 3, p. 218–234.
- Weems, R.E., and Lewis, W.C., 2002, Structural and tectonic setting of the Charleston, South Carolina, region: Evidence from the Tertiary stratigraphic record: *Geological Society of America Bulletin*, v. 114, p. 24–42, doi: 10.1130/0016-7606(2002)114<0024:SATSOT>2.0.CO;2.
- Westerhold, T., Bickert, T., and Röhl, U., 2005, Middle to late Miocene oxygen isotope stratigraphy of ODP Site 1085 (SE Atlantic): New constraints on Miocene climate variability and sea-level fluctuations: *Palaeogeography, Palaeoclimatology, Palaeoecology*, v. 217, p. 205–222, doi: 10.1016/j.palaeo.2004.12.001.
- Williams, T., and Handwerger, D., 2005, A high-resolution record of early Miocene Antarctic glacial history from ODP Site 1165, Prydz Bay: *Paleoceanography*, v. 20, PA 2017, p. 1–17, doi: 10.1029/2004PA001067.
- Wright, J.D., and Miller, K.G., 1992, Miocene stable isotope stratigraphy, Site 747, Kerguelen Plateau, in Wise, S.W., Jr., Schlich, R., et al., *Proceedings of the Ocean Drilling Program, Scientific Results, Volume 120, Part B: College Station, Texas, Ocean Drilling Program*, p. 855–866.
- Zachos, J.C., Breza, J., and Wise, S.W., 1992, Earliest Oligocene ice-sheet expansion on East Antarctica: Stable isotope and sedimentological data from Kerguelen Plateau: *Geology*, v. 20, p. 569–573, doi: 10.1130/0091-7613(1992)020<0569:EOISEO>2.3.CO;2.
- Zachos, J.C., Shackleton, N., Revenaugh, J., Pälike, H., and Flower, B., 2001, Climate response to orbital forcing across the Oligocene–Miocene boundary: *Science*, v. 292, p. 274–278, doi: 10.1126/science.1058288.

MANUSCRIPT ACCEPTED BY THE SOCIETY 3 MARCH 2009